

# TECHNICAL PAPERS

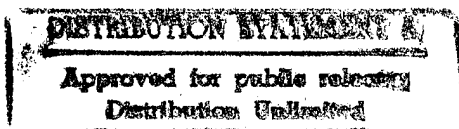
•  
PAG  
TECHNICAL CONFERENCE  
*"Design of Experiments and  
Data Analysis in Plastics  
Engineering"*

•  
SEPTEMBER 19-20, 1968  
Hermann Hall  
Illinois Institute of Technology  
Chicago, Illinois

DEPARTMENT OF DEFENSE  
PLASTICS TECHNICAL EVALUATION CENTER  
PICATINNY ARSENAL, DOVER, N. J.

SOCIETY OF PLASTICS ENGINEERS, INC.

Polymer Structure and Properties



19951107 113

DTIC QUALITY INSPECTED 8

PLASTIC

27901  
27902-27904

\*MSG DIA DROLS PROCESSING - LAST INPUT IGNORED

-- 1 OF 1

\*\*\*DTIC DOES NOT HAVE THIS ITEM\*\*\*

-- 1 - AD NUMBER: D424099  
-- 5 - CORPORATE AUTHOR: SOCIETY OF PLASTICS ENGINEERS GREENWICH CONN\*  
-- 6 - UNCLASSIFIED TITLE: DESIGN OF EXPERIMENTS AND DATA ANALYSIS IN  
-- PLASTICS ENGINEERING.  
--11 - REPORT DATE: SEP 19, 1968  
--12 - PAGINATION: 50P  
--20 - REPORT CLASSIFICATION: UNCLASSIFIED  
--21 - SUPPLEMENTARY NOTE: PROCEEDINGS: PAG TECHNICAL CONFERENCE, '  
-- DESIGN OF EXPERIMENTS AND DATA ANALYSIS IN PLASTICS ENGINEERING',  
-- 19-20 SEP 68, CHICAGO, IL. SPONSORED BY SOCIETY OF PLASTICS  
-- ENGINEERS, POLYMER STRUCTURE AND PROPERTIES PROFESSIONAL ACTIVITY  
-- GROUP. (SEE PL-27902 - PL-27904).  
--22 - LIMITATIONS (ALPHA): APPROVED FOR PUBLIC RELEASE; DISTRIBUTION  
-- UNLIMITED. ~~AVAILABILITY: SOCIETY OF PLASTICS ENGINEERS, 656 PUTNAM~~  
-- ~~AVE., GREENWICH, CT. 06030.~~  
--33 - LIMITATION CODES: 1

-- END Y FOR NEXT ACCESSION END

Alt-Z FOR HELP3 ANSI 3 HDX 3 3 LOG CLOSED 3 PRINT OFF 3 PARITY

"DESIGN OF EXPERIMENTS AND DATA ANALYSIS IN PLASTICS ENGINEERING"

PAG Technical Conference

Sponsored by

Polymer Structure and Properties

Professional Activity Group

Society of Plastics Engineers, Inc.

September 19-20, 1968

"DESIGN OF EXPERIMENTS AND DATA ANALYSIS IN PLASTICS ENGINEERING"

PAG Technical Conference of the Society of Plastics Engineers, Inc.

Sponsored by

POLYMER STRUCTURE AND PROPERTIES

PROFESSIONAL ACTIVITY GROUP

Chicago, Illinois

September 19-20, 1968

Conference Committee

Chairman	Prof. Lawrence J. Broutman	Illinois Institute of Technology
Program	Dr. Shiro Matsuoka	Bell Telephone Laboratories, Inc.
Registration	Dr. Mitsu Shida	Chemplex Company
Administrative Advisor	Leonard I. Nass	National Starch & Chemical Corp.
Chairman - Polymer Structure and Properties PAG	Dr. Thomas W. Huseby	Bell Telephone Laboratories, Inc.

Papers edited for publication by John Hyden.

Accession For	
NTIS GRA&I	<input checked="checked" type="checkbox"/>
DTIC TAB	<input type="checkbox"/>
Unannounced	<input type="checkbox"/>
Justification per	
printout enclosed	
DTIC AI	
By memo, 2 Nov 95	
Distribution/	
Availability Code	
Dist	Avail and/or
	Special
A-1	

TABLE OF CONTENTS

	<u>PAGE</u>
"Molecular Characterization of Polymers" Dr. L. H. Tung, Dow Chemical Company	1
"Flow Properties of Polymer Melts" 27902 Dr. R. A. Mendelson, Monsanto Company	7-01
"Flow Properties of PVC: Reduction to Composition and Interaction Variables" 27903 Dr. H. P. Schreiber, Canadian Industries Limited	19-02
"Some Studies of Properties of Plastics at Bell Telephone Laboratories" W. P. Slichter, S. Matsuoka, T. W. Huseby, R. S. Moore, J. H. Daane, H. E. Bair, T. K. Kwei, L. L. Blyler, Jr., and R. Salovey, Bell Telephone Laboratories	24 24
"Nonlinear Viscoelastic Characterization of Polymeric Materials" Prof. R. A. Schapery, Purdue University	42
"Aspect of Ultimate Properties: Mechanical Fatigue" 27904 George P. Koo, Allied Chemical Company	43-03

STATEMENT OF POLICY  
RELEASE FOR PUBLICATION  
OF  
REGIONAL TECHNICAL CONFERENCE PAPERS

1. All papers submitted to and accepted by the Society for presentation at one of its Regional Technical Conferences become the property of the Society of Plastics Engineers, Inc., and all publication rights are reserved by the Society.
2. The Society shall make known those papers it wishes to publish within two weeks after the close of the Regional Technical Conference at which each paper was presented.
3. The Society shall not grant previous or simultaneous publishing rights to any of the papers it intends to publish.
4. The Society shall, at the time it makes known the papers it intends to publish, release all other papers to the authors with the stipulation that, if published elsewhere, credit be given both the Society of Plastics Engineers and the specific Regional Technical Conference involved.
5. The Society shall not be responsible for statements or opinions advanced in publications, reports, papers, or in discussion at its meetings unless specifically approved by Council.
6. An abstract of any paper presented at a Regional Technical Conference may be published provided this abstract does not exceed one-third the length of the original paper as it appears in the Conference preprint. Such abstract may be published without obtaining further permission from the Society provided credit is given to both the Society of Plastics Engineers and the specific Regional Technical Conference involved.

## MOLECULAR CHARACTERIZATION OF POLYMERS

L. H. Tung

Physical Research Laboratory

The Dow Chemical Company

Midland, Michigan 48640

In the characterization of polymers, the chemical structure of the repeating monomeric units is usually known. The information of interest is the nature of the bonds linking them and the geometry of the chain structure.

Shown schematically in Figure 1 is a homopolymer, where all the repeating units are alike. For the homopolymers we would like to know the number of the repeating units in an average chain, or the average molecular weight. The chains in a sample are usually not uniform in length. We would like to know the degree of non-uniformity or the polydispersity, also the distribution of chain lengths or the molecular weight distribution of the sample. The chains may contain branches. If so, what is the average number of branches per chain, and the length of an average branch? Extensively branched chains may form crosslinked networks. What is the per cent of crosslinked networks (or gels) in a sample? What is the degree of crosslinking of the networks? In what manner are the chains linked in the network or what is the topological description of the network?

Besides the geometry of the chains, the repeating monomeric units may be linked together in more than one way. A typical vinyl-monomer is shown in Figure 2. When these monomers link together in a polymer, the carbon atom to which the group X is attached becomes asymmetrical. If the d and l configurations are arranged alternately, the chain is said to be syndiotactic. If the chain consists of only one configuration then it is isotactic. If the d and l configurations are distributed randomly, the chain is atactic.

As shown in Figure 3, the vinyl-monomers can also link up in a head-to-head configuration. For a diene type monomer there are the cis, trans and the vinyl configurations as shown in Figure 4.

For the copolymers shown in Figure 5, there are the random copolymer, the block copolymer and the graft copolymer. In a random copolymer we want to know whether the composition of all the chains is alike. In a block copolymer we want to know the block length, the number of blocks in a chain, and whether there is random copolymer mixed with the block copolymer. In a graft copolymer, we want to know the number of grafts per chain and the lengths of the grafts. The problem multiplies in complexity when we face a terpolymer. Fortunately no polymers of higher complexity than the terpolymers are of any importance in the plastics industry.

Of what have been listed above, there are some structural features which cannot be identified at the present and some others which can only be determined

approximately and with great difficulty. From a practical point of view one would like to ask whether it is necessary to know all these structural details. True enough, today, few would care to know the topology of a crosslink-network. Twenty years ago, only the rubber chemists cared anything about chain branching. The proliferation of polyethylene technology makes it a highly desirable parameter to know in the plastics industry today. In a like manner, the high-speed fabrication technique has brought forth the awareness of the importance of molecular weight distribution. Thus, it is difficult to discharge any structural feature as unimportant.

Since many properties of polymers are functions of the structure, they can be used for the characterization of the structure. One important example is the viscosity which is a function of the average molecular weight. If little or no variation is expected for the molecular weight distribution of the polymer, the melt viscosity at a given shear stress is indeed an easy method to determine the weight average molecular weight. Melt index is one such method. The melt viscosity of a polymer depends strongly on the rate of shear. This dependence is a function of the distribution of molecular weight. Thus, if a variation of molecular weight distribution is expected for the samples, a correlation of molecular weight with the zero shear viscosity must be used. A better method, however, is to use the correlation of the weight average molecular weight with the intrinsic viscosity of the polymer. Intrinsic viscosity is measured in very dilute solutions and is, therefore, relatively insensitive to the rate of shear. It can be conducted at much lower temperatures and, therefore, the danger of thermal degradation is minimized. The intrinsic viscosity requires the measurement of the reduced specific viscosity at several concentrations and the extrapolation to zero concentration as shown in Figure 6. The specific viscosity is defined by the equation

$$\eta_{sp} = \eta_r - 1 = (\eta_s/\eta_o) - 1 \quad (1)$$

where  $\eta_s$  is the viscosity of the solution and  $\eta_o$  is the viscosity of the solvent and  $\eta_r$  is the relative viscosity. The reduced specific viscosity is the ratio,  $\eta_{sp}/c$  where  $c$  is the concentration in gm/100 ml. The extrapolation can also be done through the use of inherent viscosities which is given by the group  $(\ln \eta_r/c)$ . For many polymers the variation of inherent viscosities with concentration is small and the inherent viscosity at a low concentration is often very close to the value of the intrinsic viscosity. For approximate determinations, measurement at one concentration is, therefore, sufficient.

The correlation of the intrinsic viscosity with molecular weight is given by the Mark-Houwink equation

$$[\eta] = K M^a \quad (2)$$

The constants  $K$  and  $a$  for many polymer-solvent systems are listed in the Polymer Handbook.<sup>1</sup> To calibrate these constants for an unknown polymer system, one requires the use of absolute methods of molecular weight determination, and the availability of narrow distribution polymer samples. The important methods are light scattering for the determination of weight average molecular weight, osmometry, boiling point elevation and cryoscopy for the determination of number average molecular weight. These absolute methods are not used frequently for routine work because they are difficult to perform.

Since shear rate dependence of melt viscosity depends on the distribution of molecular weight, melt indices measured at two or more shear stresses can be

used to detect the differences in polydispersity of polymer samples. Polydispersity is usually given by the ratio of weight average molecular weight to the number average molecular weight. Thus, a more direct number of polydispersity can be obtained by a measurement of the light-scattering or the intrinsic-viscosity molecular weight and another absolute measurement of the number average molecular weight. These measurements are more elaborate but the development of the high-speed membrane osmometers and the membrane-less vapor pressure osmometer has made the task easier than it was several years ago.

The polydispersity of a polymer is, of course, better characterized if the molecular weight distribution of the sample is known. The development of Gel Permeation Chromatography (GPC)<sup>2</sup> has made the determination of molecular weight distribution relatively simple as compared to the various fractionation techniques which require several days for just one determination. In GPC the separation is accomplished in a set of columns packed with porous beads made of crosslinked polystyrene or other materials. The sample is injected in the eluting solvent stream. The higher molecular weight species which penetrate the porous beads to a lesser degree are eluted out first. Today's commercial GPC units are capable of producing reliable chromatograms in about two hours. The samples can be injected at intervals shorter than the total elution time for a single sample. With the automatic sample injection device a person can often handle fifteen to twenty samples a day. The results, if interpreted correctly, are more reliable and precise than the more tedious fractionation methods. If the distribution of molecular weights is known then all the average molecular weights which are measurable through viscosity or the absolute methods of molecular weight determinations can be calculated. It appears from the reports on recent investigations<sup>3,4</sup> of GPC that a still shorter analysis time is possible for the method. The instrument can also be further automated. Thus, it is not unlikely that in a few years we may have an instrument that can produce and automatically interpret a chromatogram in about fifteen to twenty minutes' time. An on-line instrument of GPC is in the realm of possibility.

In today's GPC, depending upon the precision desired, we may use the results in perhaps three different ways. For example, in monitoring a polymerization reaction from a visual inspection of the chromatograms, we can learn whether one sample is higher or lower in molecular weight, or broader or narrower in distribution than another sample. For a more quantitative interpretation of the chromatograms, we need an accurate calibration of the elution time with molecular weight by the use of standard samples of known molecular weights. With such a calibration we can convert the chromatograms to molecular weight distribution and compute the various average molecular weights. For the most accurate interpretations, the effect of instrument spreading on the chromatograms must be considered. As in many other types of chromatography, GPC chromatograms of monomeric compounds are of finite widths. The bases of these chromatograms spread to elution volumes which correspond to both higher and lower molecular weight species. For a polydispersed sample the chromatogram is a sum of these overlapping chromatograms of the individual species in the sample. The mathematical correction of the overlapping requires a sophisticated high-speed computer and a calibration of the instrument spreading at various elution volumes. Fortunately for broad distribution samples the present available GPC instruments are capable of yielding chromatograms for which such correction is small.

Another useful method for the determination of molecular weight distribution is the sedimentation velocity measurements<sup>5</sup> by an ultracentrifuge. Initially ultra-centrifugation was developed for the characterization of biopolymers. When the centrifuge is run at a moderate speed after a certain length of time, a concentration gradient is established in the solution cell. At this time the

tendency for the solute to sediment is balanced by the tendency for it to diffuse. The latter tendency is caused by the concentration gradient. Such a technique is called equilibrium centrifugation. From it, the absolute  $z$ -average molecular weight can be calculated. If, on the other hand, centrifuge is run at a very high speed, then the solute will sediment to the bottom of the cell within a reasonable length of time. If the sample is polydispersed then the sedimentation velocity is different for the different species. From the transient concentration profile during the high speed centrifugation, the distribution of sedimentation constants may be calculated. If the relationship between the sedimentation constants and molecular weights are known, the results can be easily converted to the molecular weight distribution of the sample. The sedimentation velocity experiments require a slightly longer time to perform than GPC experiments; the requirement for the solvent is also more restrictive than that for GPC; but sedimentation velocity experiments require a slightly longer time to perform than GPC experiments; the requirement for the solvent is also more restrictive than that for GPC; but sedimentation velocity experiments do give a higher resolution than GPC for the very high molecular weight species.

When there are branches in the polymer then all the calibration relationships with molecular weight break down, the relation of intrinsic viscosity with molecular weight, the relation of elution time with molecular weight in GPC, and the relation of sedimentation constants with molecular weight in centrifugation. However, by a combination of two different measurements the degree of branching can be determined. The combination of intrinsic viscosity and light scattering or the combination of intrinsic viscosity with ultra-centrifugation is used for the detection of branches for narrow distributing samples. Drott<sup>6</sup> has used a combination of GPC and intrinsic viscosity for the determination of the average degree of branching for broad distribution polyethylene samples. It may also be possible to measure the distribution of branches as a function of molecular weight by the combination of sedimentation velocity measurement and GPC. A theory for the last method has been published,<sup>7</sup> but experimental confirmation to prove whether it may be of practical value, is still lacking.

All the above methods of branching detection are based on the fact that branching reduces the effective size of polymer chains in solution. The infrequent occurrences of long branches in the chains are significant for the rheological behavior of polymers but are untraceable by spectroscopic means. This type of branching can only be detected by these methods. The short branches which occur more frequently in low density polyethylene can be detected by infra-red spectroscopy.

Gel Permeation Chromatography and ultracentrifugation are also useful in the characterization of copolymers. For instance, Terry and Rodriguez<sup>8</sup> used an infrared spectrophotometer as the concentration detector in GPC and analyzed the copolymer of styrene and methyl-methacrylate. Other concentration detectors, such as the ultraviolet-photometer and the flame ionization detector were mentioned by them as possible means to augment the use of GPC. Ultraviolet optical system is available for use with the analytical ultra-centrifuges. The sedimentation rate in ultracentrifugation depends on the difference in density between the solvent and the polymer. By the proper choice of solvents or mixtures of two solvents, (density gradient centrifugation) many structural features of copolymers can be characterized. These ultra-centrifugation techniques are, however, still in the stage of development and are not yet used in routine characterization.

For crosslinked networks, the degree of crosslinking can be characterized by the equilibrium swell of the network by a good solvent. When a good solvent is

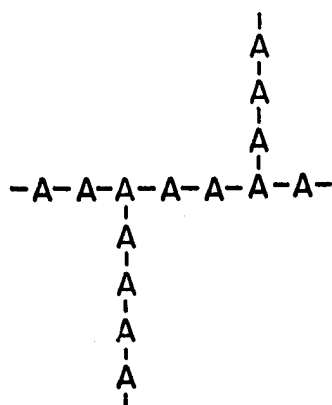
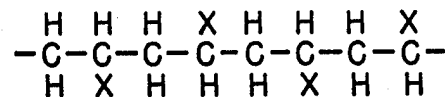
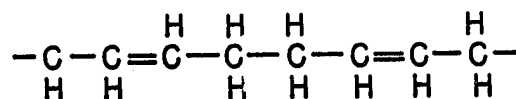
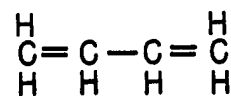
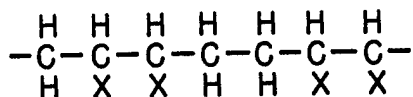
in contact with the network there is a tendency for the network to expand. This expansion is counteracted by the retracting forces developed in the expanding network. From the thermodynamics of polymer solutions, the degree of crosslink can be calculated. Other features of the network such as the distribution of chain lengths between crosslink points and the topology of the network are not characterizable at the present.

The characterization methods described so far were all developed specially for polymers. Several conventional analytical tools are also important in elucidating the structure of polymers. We have already mentioned that infrared spectroscopy can be used for the detection of branches if the number of branch points on the chains is high. Infrared spectroscopy can be used to detect the amounts of cis, trans, or vinyl double bond configurations in the chains. The tacticity of the chains can be characterized by NMR spectra. Spectra of NMR can be used to detect whether there are blocks in a copolymer chain. The proper interpretation of the data is, however, often involved and should be done by the spectroscopists.

In summary, we have shown the importance of GPC and ultracentrifugation in the characterization of polymers. We have also shown that the simple measurements of viscosity are still very much usable. The absolute methods of molecular weight determinations are used mostly in the characterization of standard samples. Many other physical-chemical methods such as differential thermal analysis, X-ray diffraction, electron microscopy, dynamic property measurements, too numerous to be included in this short report are useful for many specific structural problems. They can also be used to complement the results obtained from the methods discussed above. For a survey of the current status of polymer characterization and the outlook for future development one may consult a report published by the Materials Advisory Board.<sup>9</sup>

#### REFERENCES

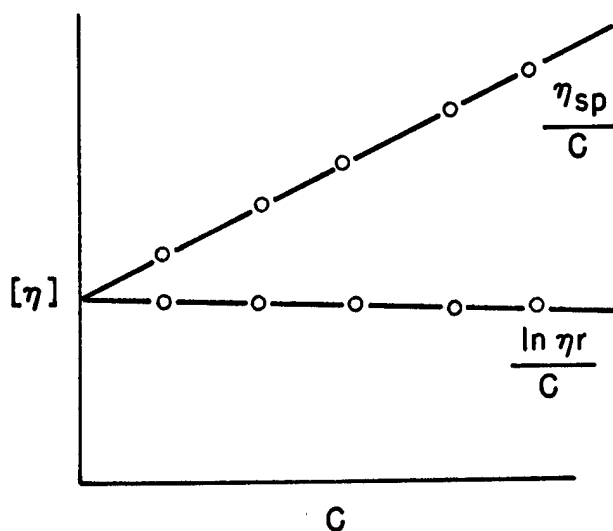
1. Polymer Handbook, ed. by J. Brandrup and E. H. Immergut, Interscience Publishers, New York, 1965.
2. Moore, J. C., J. Polymer Sci., A2, 835 (1964).
3. Le Page, M., Beau, R. and deVries, A. J., ACS Polymer Preprints, 8, 1211 (1967).
4. Billmeyer, F.W., Jr., and Kelley, R. N., ACS Polymer Preprints, 8, 1259 (1967).
5. McCormick, H. W., Chapter in Polymer Fractionation, ed. M.J.R. Cantow, Academic Press, New York, 1967.
6. Drott, E.; paper presented at the 4th International Seminar on GPC, Miami Beach, May, 1967.
7. Tung, L. H., to be published in the Journal of Polymer Science, Part A2.
8. Terry, S. L. and Rodriguez, ACS Polymer Preprints, 8, 1270 (1967).
9. Report/MAB-229-M, "Characterization of Materials", available from Clearinghouse for Federal Scientific and Technical Information, Springfield, Virginia, 22151, March, 1967.


$$\begin{array}{cc} \text{H} & \text{H} \\ | & | \\ \text{C} & = & \text{C} \\ | & | \\ \text{H} & \text{X} \end{array}$$

$$\begin{array}{cccccccc} \text{H} & \text{H} & \text{H} & \text{H} & \text{H} & \text{H} & \text{H} & \text{H} \\ | & | & | & | & | & | & | & | \\ -\text{C} & -\text{C} & -\text{C} & -\text{C} & -\text{C} & -\text{C} & -\text{C} & -\text{C}- \\ | & | & | & | & | & | & | & | \\ \text{H} & \text{X} & \text{H} & \text{X} & \text{H} & \text{X} & \text{H} & \text{X} \end{array}$$

$$\begin{array}{ccccc} & \text{H} & & \text{H} & & \text{H} \\ & | & & | & & | \\ - & \text{C} & - & \text{C} & - & \text{C} & - \\ & | & & | & & | \\ & \text{H} & & \text{CH} & & \text{H} \\ & & & || & & \\ & & & \text{CH}_2 & & \end{array}$$

$$\begin{array}{ccccccc} \text{H} & \text{H} & \text{H} & \text{H} & \text{H} & \text{H} & \text{H} \\ | & | & | & | & | & | & | \\ -\text{C} & -\text{C} & -\text{C} & -\text{C} & -\text{C} & -\text{C} & -\text{C}- \\ | & | & | & | & | & | & | \\ \text{H} & \text{X} & \text{H} & \text{X} & \text{H} & \text{X} & \text{H} \end{array}$$


```

AAAAA
  BBB

```



**FIGURE 6**

## FLOW PROPERTIES OF POLYMER MELTS

Robert A. Mendelson

Monsanto Company

Texas City, Texas 77590

The flow behavior of the polymer melt is a critical factor in determining the usefulness of a given plastics material or in determining the conditions under which that material is formed into a final product. As a consequence, both the plastics producer and the plastics engineer involved with processing resins, as well as the rheologist, have for some time concerned themselves with experiments designed to yield information about structure-melt flow relations or melt flow - extrinsic variables (e.g., temperature, flow rate, pressure, etc.) relations. A vast body of literature has, thus, developed concerning methods of measuring the melt rheological, or flow, properties of polymers and the results obtained (see, for example, the Bibliography and Special References.)<sup>1</sup> It is not the purpose of this article to attempt to summarize all of the aspects of this area, but rather to examine two specific research problems in order to illustrate two dissimilar experimental programs involving melt rheology.

[The first of these concerns the relationship of the melt viscosity of polyethylene with shear rate, or flow rate, and with temperature.] This program was initiated because it was desired to study the effect of shear refining of polyethylene in extrusion, and for this it was necessary to design a series of extruder screws which would provide a variety of shear stress levels in the metering sections for various shear rates. The shear rates could readily be approximated as a function of screw speed and geometry. The problem was to predict the corresponding shear stresses generated at the various shear rates and temperatures for a large number of resins.

The second, and quite different, experimental program involves the quantitative determination of the effect of long-chain branching (LCB) in low density polyethylene (LDPE) on melt viscosity and melt elasticity, independent of the effects of other molecular variables.] This problem arises as a consequence of the fact that in tailoring the structure of polymeric materials to have optimum flow properties it is ultimately necessary to understand the dependence of melt viscosity and melt elasticity on individual molecular structural parameters.

### TEMPERATURE AND SHEAR RATE DEPENDENCE

Two factors were significant in designing an experimental program to solve the problem of obtaining shear stress data as a function of shear rate and temperature for a large number of resins. First, the experiments would not be limited by available quantity of sample. This was in marked contrast to the considerations in solving the problem of the effect of LCB. Second, a result

having the broadest application, yet requiring the least amount of data for its use was desired. Thus, while various investigators<sup>2-6</sup> had shown in general, that the temperature dependence of the viscosity of polyethylene could be expressed in terms of an Arrhenius equation

$$\eta = A \exp (E\eta / RT) \quad (1)$$

it was not clear at the time of this investigation what the shear rate or shear stress dependence of the flow activation energy,  $E\eta$ , was or how  $E\eta$  depended upon molecular structure. Moreover, the pre-exponential constant,  $A$ , is dependent upon shear rate and molecular considerations, so that these constants would have to be measured for each polymer to be tested if this means of predicting melt viscosity as a function of shear rate and temperature were to be employed. A more general result such as superposition of flow curves (to be discussed in detail later) was required.

#### A. Experimental

Melt viscosity data discussed in this investigation were obtained for commercial samples of six LDPEs and four high density polyethylenes (HDPE), as well as one experimentally polymerized LDPE. The LDPE resins, in particular, were chosen to have a broad range of molecular and physical test properties so that the results of the study would have the most general application. Number average molecular weights,  $\bar{M}_n$ , were determined by membrane osmometry in p-xylene at 105°C, while weight average molecular weights,  $\bar{M}_w$ , were obtained by solution light scattering techniques using 1,2,3,4-tetrahydronaphthalene (tetralin) as solvent. Light scattering measurements were made either at 81.5°C with a Brice-Phoenix photometer using 436 mμ unpolarized incident light or in a Sofica instrument at 105°C using 546 mμ unpolarized incident light. Values of  $dn/dc$  used were, respectively, -0.0887 and -0.069.<sup>7</sup>  $\bar{M}_w$ s were calculated by both the Zimm and dissymmetry methods, and the molecular data along with melt index and room temperature density are given for the samples in Table I. These results have been reported previously.<sup>8</sup>

All of the melt flow data reported here were obtained using an Instron Capillary Rheometer of Monsanto design.<sup>9-11</sup> This instrument consists of an electrically thermostatted barrel, or reservoir, in the bottom of which is inserted one of a number of interchangeable capillaries. A plunger coupled to the crosshead of the Instron testing machine drives polymer melt through the capillary at a series of fixed velocities, and the force necessary to sustain this flow at each velocity is measured by means of a compression load cell. In all cases studied here a capillary with a large length-to-ratio (L/D) was used, eliminating the need for entrance-effect corrections to the shear stress, and in all cases but one the capillaries used had the following nominal dimensions: 0.06 inch diameter, 4.0 inch length, and 90° included entry angle. The shear rate range covered was in general 0.17-1700 sec<sup>-1</sup>. The temperature ranges were 120-300°C for LDPE and 150-300°C for HDPE. Thus, the factor mentioned earlier, the availability of a sufficient quantity of sample in all cases but one (MAC-4) made it possible to obtain experimental data over a very extensive range of shear rates and temperatures.

The basic quantities measured in such a capillary rheometer are the linear plunger velocities which are directly related to the volumetric flow rates,  $Q$ , through the capillary, and the driving forces,  $F$ . Shear stresses and shear rates at the wall may then be calculated from the measured flow data using the expressions for Newtonian flow in cylindrical capillaries:

$$\tau_w = PR/2L \quad (2)$$

and 
$$\dot{\gamma}_w = 4Q/\pi R^3 \quad (3)$$

where  $P$  is the pressure drop across the capillary of radius  $R$  and length  $L$ , and is given by the force,  $F$ , per unit plunger (cross-sectional) area,  $A$ . It has already been noted that all experiments were performed using high  $L/D$  ratio capillaries such that end-effects were negligibly small, i.e.,  $\tau_w$  may be considered to be the true shear stress at the wall, and  $P$  calculated as indicated is the actual pressure drop in the capillary. In order to obtain the true shear rate at the capillary wall it is necessary to apply a correction<sup>12</sup> for the non-Newtonian character of the flow. However, because of a desire to apply as few curve-fitting procedures to the data before testing the validity of superposition as possible and because it can be shown that, where shear rate-temperature superposition applies, the Rabinowitsch correction to the shear rate does not alter the values of the shift factors obtained, the "apparent" shear rates calculated by Equation 3 were used throughout this work. Thus, the apparent viscosity is given at each shear rate as

$$\eta_a = \tau_w / \dot{\gamma}_w \quad (4)$$

Typical flow curves ( $\log \tau_w$  vs.  $\log \dot{\gamma}_w$ ) at temperatures from 120°C to 300°C are shown in Figure 1 for LDPE Sample A. Similar curves were obtained for all samples.

## B. Results

It was found that, for each sample, these flow curves at the various temperatures could be shifted along the shear rate axis, to superimpose on a single master curve for that sample, where the master curve corresponded to the flow curve for the arbitrarily chosen reference temperature of 200°C. The amount by which each curve had to be shifted in order for it to superimpose on the 200°C curve is known as the shift factor. These horizontal shift factors  $a_T$  were, in the case of each sample studied, obtained by choosing the shear stresses at 10 and 30 sec<sup>-1</sup> on the 200°C flow curve and shifting the corresponding (constant shear stress) points on the flow curves at the other temperatures  $T$  to coincide with these shear rates. The values of  $a_T$  were calculated from

$$a_T = \dot{\gamma}_w(\text{ref.}) / \dot{\gamma}_w(T) \quad (\text{const. } \tau_w) \quad (5)$$

and, for each temperature, the values of  $a_T$  corresponding to 10 and 30 sec<sup>-1</sup> at the reference temperature were averaged to reduce errors due to reading of graphs.

Values for  $a_T$  as a function of temperature are given in Tables II and III for three HDPE and five LDPE samples, respectively. It may be seen that, while a considerable amount of experimental error exists, there is no dependence of shift factor on molecular weight or molecular weight distribution. Thus, it was possible to obtain an averaged unique set of shift factors for all HDPE samples and a second unique set for all LDPE samples. In order to test the applicability of these shear rate-temperature superposition shift factors, the averaged  $a_T$ s were used to construct master flow curves at 200°C utilizing Equation 5. A number of the resultant master curves are shown in Figures 2 and 3 and clearly illustrate the general validity of the superposition method.

The temperature dependence of the shift factors was next investigated, and a simple exponential, or Arrhenius-type, equation of the form

$$a_T = B \exp (E_a/RT) \quad (6)$$

where  $T$  is the absolute temperature and  $E_a$  is the "shift factor activation energy", was found to give an excellent fit for each of the polymer systems (i.e., HDPE and LDPE) over the appropriate temperature ranges covered, as shown in Figure 4. Values of  $E_a$  were found to be 6.3 kcal/mole for HDPE and 11.7 kcal/mole for LDPE. Substituting the constants derived from a least-squares fitting of the data, Equation 6 may be rewritten in logarithmic form for each type polymer as follows:

$$\text{(HDPE)} \quad \log a_T = -2.950 + 1.39 \times 10^3 (1/T) \quad (6a)$$

and

$$\text{(LDPE)} \quad \log a_T = -5.415 + 2.55 \times 10^3 (1/T) \quad (6b)$$

### C. Flow Curve Prediction

The foregoing experimental results provide the basis for a rather general technique for predicting melt viscosity flow curve data at various temperatures. It is apparent that Equation 5 may be rewritten in terms of the shear rate at any temperature,  $T$ , as follows

$$\dot{\gamma}_w(T) = \dot{\gamma}_w(\text{ref.})/a_T \quad (7)$$

where the corresponding shear stress is the same at the two shear rates. Thus, given a set of shear stress-shear rate data at the reference temperature and a knowledge of  $a_T$  as a function of temperature, it is possible to construct sets of  $\tau_w$ - $\dot{\gamma}_w$ - $\eta_a$  data at any desired temperature. Moreover, it is not even necessary that the known data set be available at the reference temperature since, assuming data to be known at  $T_1$  and desiring data at  $T_2$ , elimination of  $\dot{\gamma}_w(\text{ref.})$  from Equation 5 yields

$$\dot{\gamma}_w(T_2) = a_{T_1} \dot{\gamma}_w(T_1)/a_{T_2} \quad (8)$$

Appropriate values of  $a_T$  are obtained from Equations 6a or 6b.

As an illustration of the use of this technique in predicting flow curves, melt flow data were obtained at 150°C and 200°C for two LDPE samples (M and N) which had not been used in the studies developing the technique or the shift factor values. The 150°C flow curves for the two samples were calculated by superposition from the 200°C data and are shown in Figure 5 along with the actually measured 150°C data. The agreement is seen to be excellent. It should be pointed out that this technique is ideally suited for computer utilization<sup>13</sup> if data at large numbers of temperatures are desired.

#### DEPENDENCE OF VISCOSITY AND ELASTICITY ON LCB

The problem of obtaining quantitative information about the effect of LCB on the melt viscosity and melt elasticity of LDPE has been compounded by the difficulty of determining the amount of LCB present in a given sample and by the extreme difficulty of separating the effects of molecular weight, molecular weight distribution, and LCB both for the determination of branching and for defining its effect on melt rheology. Thus, while some attempts<sup>14-16</sup> have been made to establish the relationship between LCB and melt viscosity in LDPE, they have not been totally successful, and little is known experimentally about the effect on melt elasticity.

The experimental problem here was quite different from the one described earlier. Here the important point was to separate the molecular structure variables so that all but LCB could be held constant while LCB was varied in a systematic fashion over a series of samples. This required that the samples be prepared either by careful fractionation of several different materials or by equally careful polymerization. In either case only relatively small amounts of polymer could be provided. Thus, the method of rheological investigation had to be adapted to small samples, as well. In the experimental investigation described rather briefly here samples were provided by free radical polymerization of two polyethylenes in an isothermal, isobaric autoclave reactor such that both molecular weight level and molecular weight distribution were essentially the same for the two samples, but the degree of LCB was varied. Portions of these samples were then blended to make two additional samples so that, in all, four materials of differing branching level, but constant molecular weight parameters, were available.

#### A. Experimental

$\bar{M}_n$  and  $\bar{M}_w$  values of the two polymerized samples were determined by high speed membrane osmometry (o-dichlorobenzene solvent, 135°C) and solution light scattering (Sofica instrument, 1-chloronaphthalene solvent, 125°C, 546 mμ wave length,  $dn/dc = 0.195$ ),<sup>7</sup> respectively. Table IV shows the results for these samples, MAB-1112A and MAB-1112D, to be essentially identical. Thus, the  $\bar{M}_n$  and  $\bar{M}_w$  values for the blended samples, MAB-1112B and MAB-1112C, are also shown in the table as equal to those of the A and D samples. Intrinsic viscosities were measured in p-xylene at 105°C for the A and D samples and were calculated from the relation

$$[\eta] = \sum w_i [\eta]_i \quad (9)$$

for the B and C samples.

The LCB of these samples were determined by relating the intrinsic viscosity of the branched material to that of a linear material of the same molecular weight. Thus, a branching index,  $g$ , was calculated from

$$g^{1/2} = [\eta]_{br}/[\eta]_l \quad (10)$$

where  $[\eta]_{br}$  is the measured intrinsic viscosity for the branched sample, and  $[\eta]_l$  for the linear polymer of the same molecular weight is derived from Tung's<sup>17</sup> equation for linear polyethylene in tetralin at 130°C.

$$[\eta]_l = 4.60 \times 10^{-4} \bar{M}_w^{0.725} \quad (11)$$

(Previous unpublished work in this laboratory showed that  $[\eta]$  (p-xylene, 105°C) =  $[\eta]$  (tetralin, 130°C)). The branching index,  $g$ , was then related to the weight average number of long-chain branches per molecule,  $\bar{n}_w$ , according to the theory of Zimm and Stockmayer<sup>18</sup> by the equation

$$\langle g \rangle_w = \frac{6}{\bar{n}_w} \left[ \frac{1}{2} \left( \frac{2 + \bar{n}_w}{\bar{n}_w} \right)^{1/2} \ln \left\{ \frac{(2 + \bar{n}_w)^{1/2} + \bar{n}_w^{1/2}}{(2 + \bar{n}_w)^{1/2} - \bar{n}_w^{1/2}} \right\} - 1 \right] \quad (12)$$

Values of  $\bar{n}_w$  so obtained are given in Table IV.

Melt viscosity and melt elasticity data were obtained using a Weissenberg Rheogoniometer.<sup>19</sup> Details of this commercially available instrument and its operation will not be discussed here. However, the instrument is basically a cone-and-plate-rheometer capable of measuring the principal normal stress difference as well as the shear stress. Thus, both viscous and elastic properties of the molten sample may be evaluated in either mode of operation. This instrument, rather than a capillary rheometer, was chosen for this investigation because of this capability for measuring a number of rheological parameters and because it requires only relatively small samples (ca. 0.5 gram per measurement in our case). All samples were stabilized with Santonox R prior to testing, and all measurements were made at 150°C. Values of shear stress,  $\tau$ , and normal stress difference,  $(p_{11} - p_{22})$ , were determined as a function of shear rate in the steady rotational experiments, and values of the complex viscosity,  $\eta^*l$ , the dynamic viscosity,  $\eta'$ , and the elastic "storage" modulus,  $G'$ , were determined as a function of frequency in the oscillatory experiments.

## B. Results

In this discussion, only a limited number of resulting flow parameters will be considered. (A more detailed account of this investigation will be presented elsewhere.) The low shear Newtonian limiting viscosities of all four samples were obtained and were found to coincide with the limiting low frequency values of the complex viscosity. The onset of non-Newtonian behavior, taken as the shear rate at which the apparent viscosity had decreased to 95% of its Newtonian value,  $\dot{\gamma}(95\% \eta_0)$ , was observed as a measure of shear sensitivity of the viscosity, and the

elastic storage modulus,  $G'$ , measured at 10 rad/sec was taken as a measure of the melt elasticity of the materials. These quantities are given in Table V. Moreover, the limiting viscosity and the elastic storage modulus at 10 rad/sec are shown as a function of the number of long-chain branches per molecule in Figure 6.

The effect of LCB independent of molecular weight and molecular weight distribution may be clearly seen in Table V and Figure 6. Both limiting melt viscosity and melt elasticity decrease for these materials as the number of branches increases. Moreover, the viscosity becomes non-Newtonian, i.e., shear sensitive, at lower shear rates the greater the number of branches. To confirm the effect of branching on melt elasticity the elastic recoverable shear strain was calculated from the steady shear data according to the equation

$$\gamma_r = (p_{11} - p_{22})\tau \quad (13)$$

and smoothed curves of  $\gamma_r$  vs.  $\dot{\gamma}$  are shown in Figure 7, confirming that at a fixed shear rate the elasticity decreases with increasing branching.

## SUMMARY

The foregoing discussion was meant to illustrate some of the factors which go into the design of experiments required to solve problems in the field of plastics. Two quite diverse problems were considered. In the first case a series of experiments were described which provided a very general technique for predicting polyethylene flow behavior as a function of shear rate over a wide range of temperatures from a minimum of new data. In this case the experimentation concerned only the viscous aspect of flow and was not limited by the availability of special samples. In the second case it was desired to learn what the effect of a specific molecular structural variable was on the general melt rheological properties of polyethylene. This required the polymerization of special samples followed by detailed characterization by both solution property and melt rheological techniques.

## REFERENCES

1. Mendelson, R.A., "Melt Viscosity", Encyclopedia of Polymer Science and Technology, Vol. 8, H. F. Mark, N. G. Gaylord, N. M. Bikales, (eds.), Interscience Publishers, New York, in press.
2. Philippoff, W. and Gaskins, F. H., J. Polymer Sci., 21, 205 (1956).
3. Aggarwal, S. L., Marker, L. and Carrano, M. J., J. Appl. Polymer Sci., 3, 77 (1960).
4. Porter, R. S. and Johnson, J. F., J. Appl. Polymer Sci., 3, 194 (1960).
5. Schott, H. and Kaghan, W. S., J. Appl. Polymer Sci., 5, 175 (1960).

#### REFERENCES (Cont'd.)

6. Westover, R. F., "Processing of Thermoplastic Materials", Section III, E. C. Bernhardt (ed.), Reinhold Pub., New York, 1959, pp. 590-627.
7. Drott, E. E. and Mendelson, R.A., J. Polymer Sci., B2, 187 (1964).
8. Mendelson, R. A., Trans. Soc. Rheol., 9:1, 53 (1965); Polymer Eng. and Sci., in press.
9. Merz, E. H. and Colwell, R. E., ASTM Bull. 232, 63 (1958).
10. Ballman, R. L. and Brown, J. J., Instron Applications Series SA-2 (1961).
11. Van Wazer, J. R., Lyons, J. W., Kim, K. Y. and Colwell, R.E., "Viscosity and Flow Measurement", Interscience, New York, 1963, pp. 231 ff.
12. Rabinowitsch, B., Z. Physik. Chem., A145, 1 (1929).
13. Mendelson, R. A., Ch. 2.4 in Computer Programs for Plastics Engineers, D. I. Marshall and I. Klein (eds.), Reinhold Pub., New York, to be published.
14. Moore, L. D., Jr., J. Polymer Sci., 36, 155 (1959).
15. Tung, L. H., J. Polymer Sci., 46, 409 (1960).
16. Schreiber, H. P. and Bagley, E. B., J. Polymer Sci., 58, 29 (1962).
17. Tung, L. H., J. Polymer Sci., 36, 287 (1959).
18. Zimm, B. H. and Stockmayer, W. H., J. Chem. Phys., 17, 130 (1949).
19. Ref. 11, pp. 113 ff.

TABLE I  
POLYETHYLENE SAMPLE CHARACTERISTICS

<u>Sample</u>	<u>MI</u>	<u>Density</u>	<u><math>\bar{M}_n \times 10^{-3}</math></u>	<u><math>*M_w \times 10^{-3}</math></u>	<u><math>*M_w/\bar{M}_n</math></u>
HDPE					
1	0.8	0.963	32.1	200	6.2
2	0.2	0.962	39.4	313	7.9
3	0.23	0.951	36.9	253	6.9
4	0.24	0.948	--	--	--
LDPE					
A	6.9	0.918	27.4	730	27
B	1.2	0.920	27.3	1240	45
C	0.23	0.918	34.2	1580	46
D	2.1	0.929	37.8	230	6.1
MAC-4	--	0.939	28.6	55.6	1.9
M	0.25	0.918	--	--	--
N	1.3	0.917	--	--	--

$*M_w$  calculated by dissymmetry.

TABLE II

HDPE

\*SHIFT FACTOR VALUES FOR 200°C REFERENCE TEMPERATURE

<u>Temperature</u> <u>°C</u>	<u>at</u>		
	<u>Sample 1</u>	<u>Sample 2</u>	<u>Sample 3</u>
150	2.08	2.17	2.23
175	1.37	1.46	1.47
200	1.00	1.00	1.00
225	0.679	0.706	0.738
250	0.523	0.543	0.523
275	0.368	0.430	0.399
300	0.298	0.306	0.277

\*Taken from Ref. (8)

TABLE III

## LDPE

\*SHIFT FACTOR VALUES FOR 200°C REFERENCE TEMPERATURE

Temperature (°C)	$a_T$				
	Sample A	Sample B	Sample C	Sample D	Sample MAC-4
120	11.5	11.1	12.3	11.9	--
125	--	--	--	9.73	--
130	--	--	--	--	7.54
150	4.16	3.79	3.91	3.81	4.05
175	1.75	1.81	1.97	1.87	--
200	1.00	1.00	1.00	1.00	1.00
250	0.289	0.277	0.323	0.317	--
275	--	--	--	0.179	--
300	0.0979	0.0971	0.0967	0.0993	--

\*Taken from Ref. (8).

TABLE IV

## MOLECULAR PROPERTIES OF LDPE BRANCHING STUDY SAMPLES

Sample	Composition	$[\eta]$ (dl/g)	$\bar{M}_n$ $\times 10^{-3}$	$\bar{M}_w$ $\times 10^{-3}$	$\bar{M}_w/\bar{M}_n$	$\bar{n}_w$
MAB-1112A	100% A	0.627	27.3	42.5	1.6	13.0
MAB-1112B	74.9%A; 25.1%D	0.708	27.0	43.0	1.6	8.3
MAB-1112C	34.0%A; 66.0%D	0.841	27.0	43.0	1.6	4.0
MAB-1112D	100%D	0.951	26.8	43.0	1.6	1.5

TABLE V

## MELT RHOLOGICAL RESULTS OF BRANCHING STUDY

Sample	$\eta_0$ (poise)	$\eta^*_{1w \rightarrow 0}$	$\dot{\gamma}(95\% \eta_0)$ (sec <sup>-1</sup> )	$G'$ (10 rad/sec) (dynes/cm <sup>2</sup> )
MAB-1112A	$2.5 \times 10^3$	$2.5 \times 10^3$	$2.0 \times 10^1$	$3.2 \times 10^3$
MAB-1112B	$6.6 \times 10^3$	$6.6 \times 10^3$	$4.5 \times 10^0$	$1.4 \times 10^4$
MAB-1112C	$2.45 \times 10^4$	$2.5 \times 10^4$	$6.2 \times 10^{-1}$	$6.7 \times 10^4$
MAB-1112D	$6.3 \times 10^4$	$6.3 \times 10^4$	$3.0 \times 10^{-1}$	$1.4 \times 10^5$

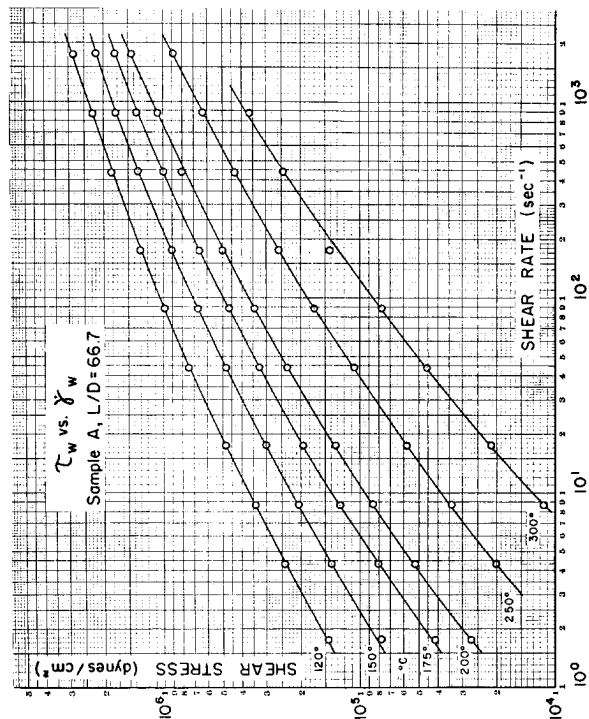


FIGURE 1: Shear stress vs. shear rate flow curves for LDPE Sample A at six temperatures.

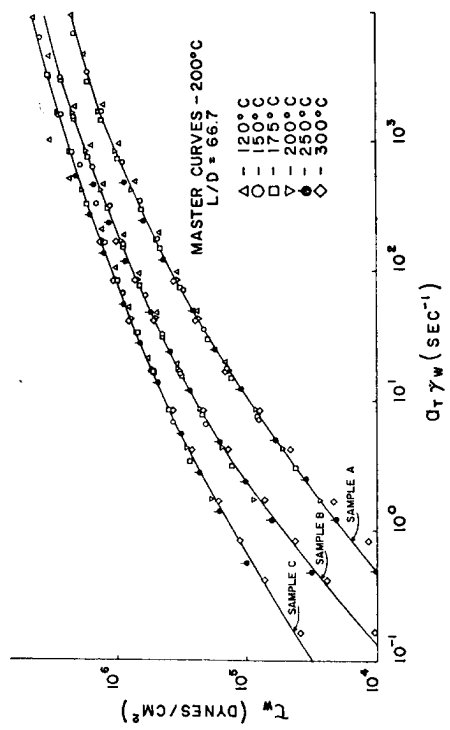


FIGURE 2: Superposition master flow curves (200°C ref. temp.) for LDPE Samples A, B, and C.

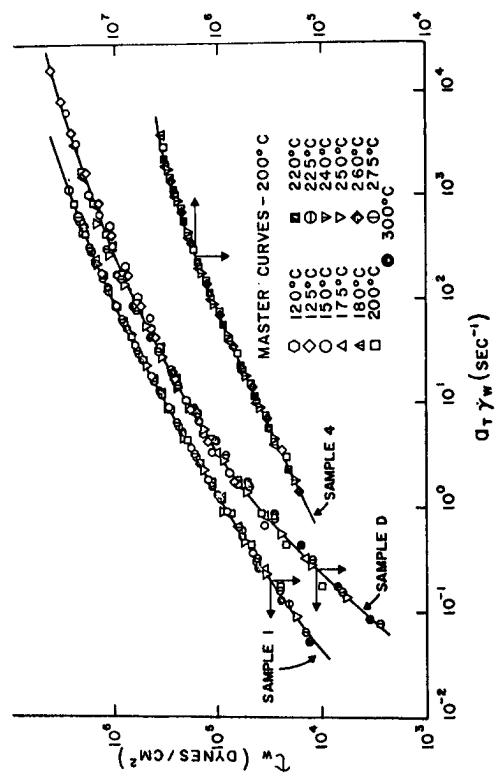


FIGURE 3: Superposition master flow curves (200°C ref. temp.) for LDPE Sample D and HDPE Samples 1 and 4.

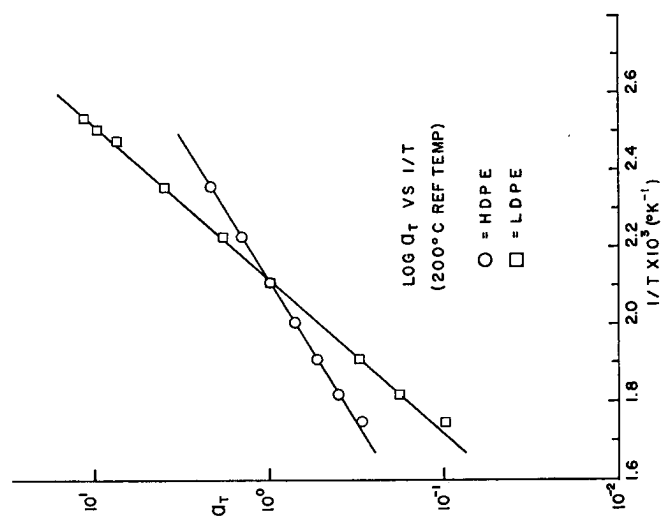


FIGURE 4: Temperature dependence of superposition shift factors.

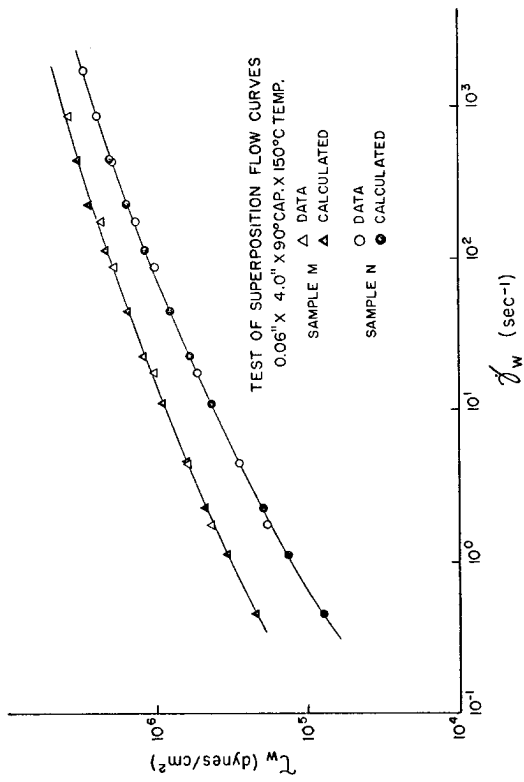


FIGURE 5: Test of superposition method comparing calculated and measured flow curves for LDPE Samples M and N.

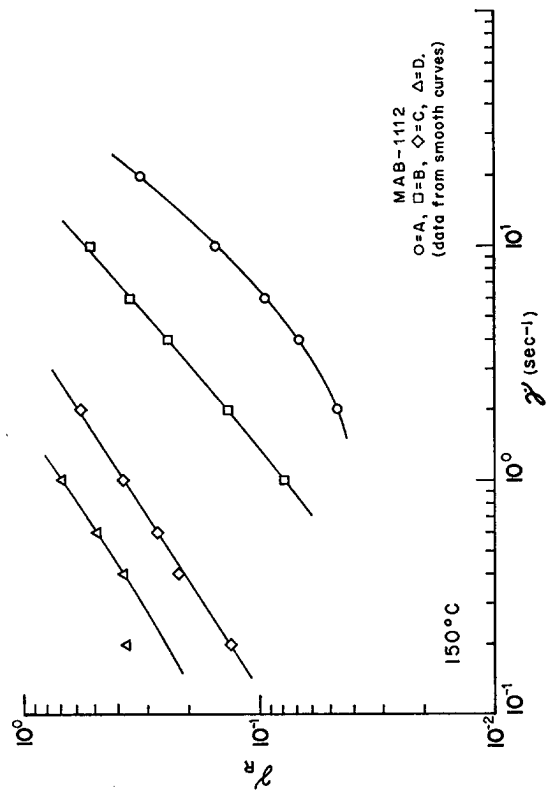


FIGURE 7: Recoverable elastic shear strain vs. shear rate as a function of LCB (150°C).

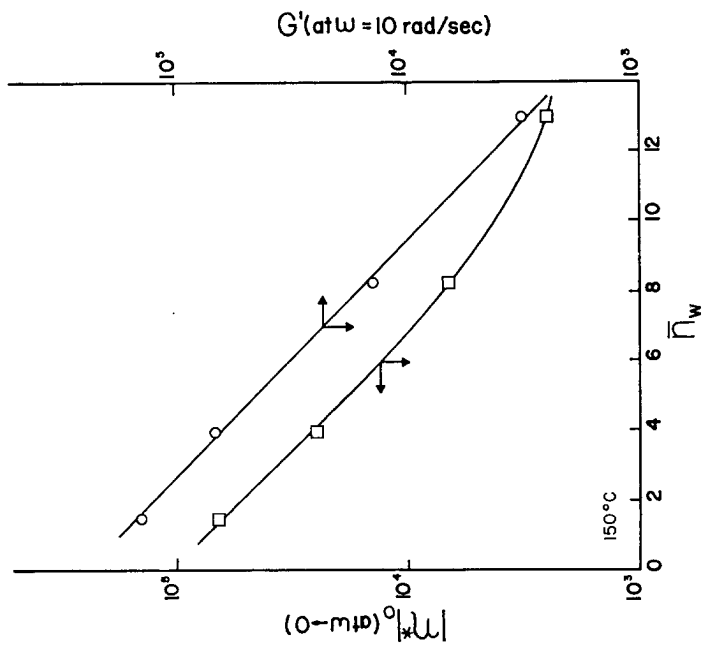


FIGURE 6: Limiting viscosity and storage modulus (at 10 rad/sec) vs. number of long-chain branches per molecule, MAB-1112 series (150°C).

02

FLOW PROPERTIES OF PLASTICIZED PVC:  
REDUCTION TO COMPOSITION AND INTERACTION VARIABLES

H. P. Schreiber

Central Research Laboratory  
Canadian Industries Limited  
McMasterville, Que., Canada

INTRODUCTION

~~The flow behaviour of PVC compounds is complicated by the large variety of additives normally mixed with the polymer.~~ In this paper an attempt is made to rationalize the flow properties of model, plasticized PVC compounds, by applying widely recognized concepts of polymer rheology and polymer-diluent interaction. The approach can be regarded as a first step to a more general rationalization, permitting precalculation of the flow properties of given compounds over temperature and shear rate ranges of practical interest from a knowledge, principally, of plasticizer volume fraction and the value of a polymer-plasticizer interaction parameter.

J. Caution

EXPERIMENTAL

This work used compounds made up from two PVC polymers having  $[\eta]$  values in tetrahydrofuran of 1.03 and 1.16 dl/gm., and diisooctyl phthalate (P series), 6-10 adipate (A series) and a 50/50 mixture of these plasticizers (P/A series of compounds). An organo-tin stabilizer and calcium stearate lubricant were present in proportions shown in Table I, where  $\phi_1$  is the volume fraction of plasticizer present in the compounds. All the compounds were fused by roll-milling prior to extrusion, so as to eliminate particle boundaries recently discussed by Berens and Folt<sup>1,2</sup> and thus simplify the flow behaviour. Flow data were obtained in the temperature range 150°-200°C., using the C-I-L High Shear Viscometer fitted with a die with  $L/R = 7.64$ . Typical flow curves are shown in Figure 1 for phthalate-plasticized compounds at 165°C. Similar sets of such curves were obtained for each plasticizer series at each melt temperature. The plots were used to construct corresponding graphs of log melt viscosity vs. polymer volume fraction ( $\phi_2 = 1 - \phi_1$ ). The resulting set of nearly linear functions was used to extrapolate the melt viscosity of unplasticized polymer ( $\phi_2 = 1$ ). The resulting viscosity-shear rate diagram for one of the polymers is shown in Figure 2. Evidently, the very distinct flow curves of the variously plasticized polymer nicely define the behaviour of the unplasticized matrix at each of the experimental temperatures and over several decades of shear rate.

## REDUCED VARIABLE TREATMENT

The unique flow curves derived for unplasticized PVC from the flow data of plasticized compounds, indicated that master curves for various levels of plasticization could be constructed by a reduced variable treatment. The approach used was that of Kraus and Gruver,<sup>3</sup> which applies concepts due to Bueche<sup>4</sup> to dilute polymer mixtures, and which defines shift factors for the translation of points on the flow curves of plasticized compounds to points on the corresponding curve of the unplasticized polymer. In theory the shift factor,  $a\phi$ , equals the ratio of Newtonian (zero-shear) viscosities of plasticized and unplasticized polymer. The reduced variable treatment produced master flow curves of  $\log \eta/a\phi$  versus  $\log \dot{\gamma} a\phi/\phi_2^2$ . These closely define the rheology of compounds at given temperature over a broad shear rate range and for plasticization levels up to 60 phr. of each of the three plasticizer systems used. A typical master curve for polymer I is shown in Figure 3.

## RESULTS OF REDUCED VARIABLE TREATMENT

The most apparent result is the demonstration that if the flow curve of a parent PVC polymer is known then knowledge of the volume fraction of polymer in a compound and of the corresponding  $a\phi$  is sufficient to precalculate a broad range of viscosity-shear rate data. It was further shown that for a given plasticizer at given temperature, the shift factor is a simple function of plasticizer volume fraction, following the equation

$$\log a\phi = -k_T (1 - \phi_2) \quad (1)$$

where  $k_T$  is a temperature dependent constant. The same relationship applied to compounds of both PVC polymers using a given plasticizer. Thus, the relationship may apply generally to fused PVC compounds employing a specific plasticizer or plasticizer mixture.

Analysis of the slopes of  $\log a\phi$  vs.  $\phi_2$  plots showed that these could be related to the absolute temperature,  $T$ , via

$$k_T = A + B \left( \frac{1}{T} \right) \quad (2)$$

The equation for each plasticizer system applies only in the investigated temperature span (150°-200°C.), but indicates the feasibility of applying temperature corrections for known  $a\phi$  values within this practically useful range. Thus, for specific plasticizer systems, a generalized approach to plasticizer volume and melt temperature dependence of  $a\phi$  has been outlined.

## INFLUENCE OF POLYMER-DILUENT INTERACTION

Inspection of shift factor values and of the  $k_T$  slopes indicated a strong dependence on the type of plasticizer used. A path was, therefore, suggested for the correlation of actual values of these parameters with values of a polymer-plasticizer interaction parameter. The Flory-Huggins interaction parameter  $\chi$  for the phthalate, adipate and mixed plasticizer systems was determined using the photographic technique of Anagnostopoulos and coworkers.<sup>5,6</sup> Because of the conditions employed by this method, the  $\chi$  value is strictly valid only for high levels of plasticization and at temperatures near the reduced melt temperature of the highly

plasticized polymer - in general, lower than the range used for rheological measurements. Within this limitation, however, the existence of a correlation between the two sets of parameters was successfully demonstrated, as shown in Figure 4. The quotient  $\alpha\phi/\phi^{3.4}$  was used to represent the rheological factor since the magnitude of deviations from unity in this value best indicate the importance of polymer-diluent interactions.<sup>3</sup> The correlation in Figure 4 shows that it is possible to precalculate  $\alpha\phi$  values from literature or experimental values of  $\chi$ , and that for a given polymer the upper limit of  $\chi$  can be defined at which  $\alpha\phi/\phi^{3.4} \rightarrow 1$ . Plasticizers having  $\chi$  greater than this limit will, therefore, contribute only volume dilution effects to the viscosity of plasticized compounds. This work, therefore, shows that provided adequately accurate interaction values are available ( $\chi$  is known to be a function both of temperature and diluent concentration), then precalculation of  $\alpha\phi$  over wide temperature, shear and plasticization level ranges should be possible and hence also the corresponding prediction of flow curves for plasticized PVC compounds. The necessary specification of  $\chi$  values is worthy of serious consideration by industrial research units.

#### REFERENCES

1. Berens, A.R. and Folt, V.L., Poly. Eng. Sci. 8, 5 (1968).
2. Berens, A.R. and Folt, V.L., Trans. Soc. Rheology 11:1, 95 (1967).
3. Kraus, G. and Gruver, J. T., Trans. Soc. Rheology 9:2, 17 (1965).
4. Bueche, F., J. Appl. Phys. 30, 1114 (1959).
5. Anagnostopoulos, C.E., Coran, A.Y. and Gamrath, H.R., J. Appl. Polymer Sci. 4, 181 (1960).
6. Anagnostopoulos, C.E. and Coran, A.Y., J. Polymer Sci. 57, 1 (1962).

TABLE I

COMPOSITION OF PVC SAMPLES USED IN FLOW STUDIES

SAMPLE NO:		<u>1</u>	<u>2</u>	<u>3</u>	<u>4</u>	<u>5</u>
Resin	(phr)	100	100	100	100	100
Stabilizer	(phr)	3	3	3	3	3
Ca Stearate	(phr)	1	1	1	1	1
Plasticizer	(phr)	15	25	40	50	60
$\phi_1$	P series	0.177	0.263	0.363	0.416	0.461
	A series	0.188	0.278	0.382	0.435	0.481
	P/A series	0.182	0.271	0.372	0.426	0.471

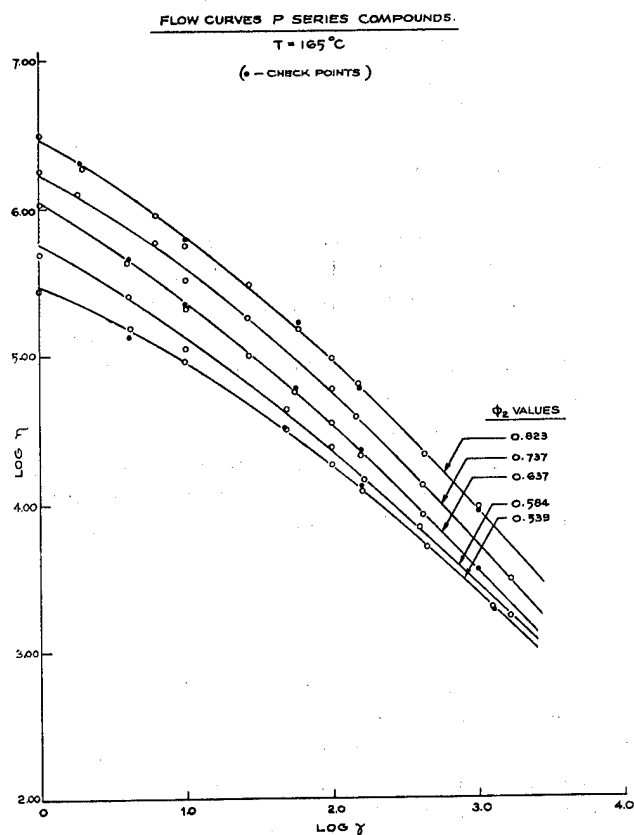


FIGURE 1

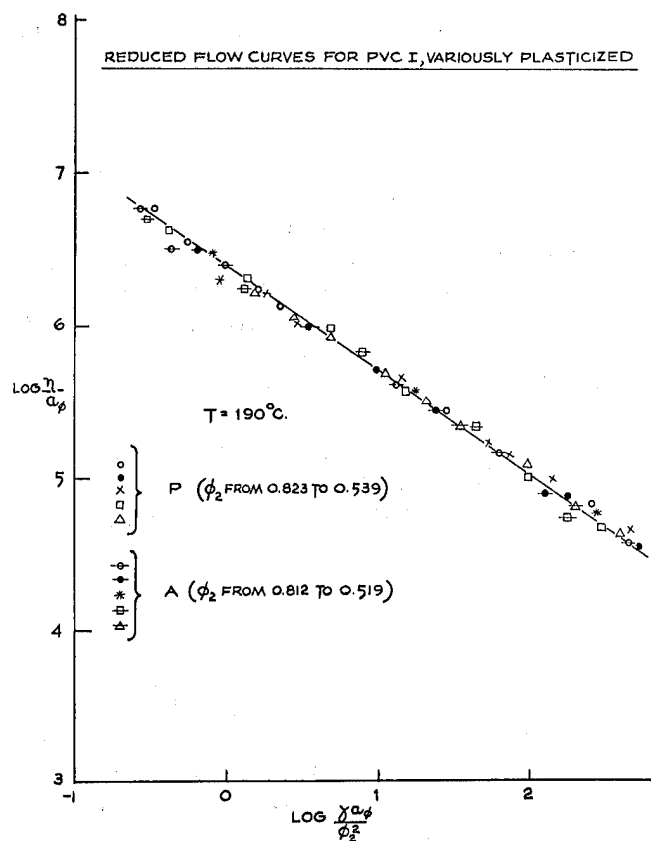


FIGURE 3

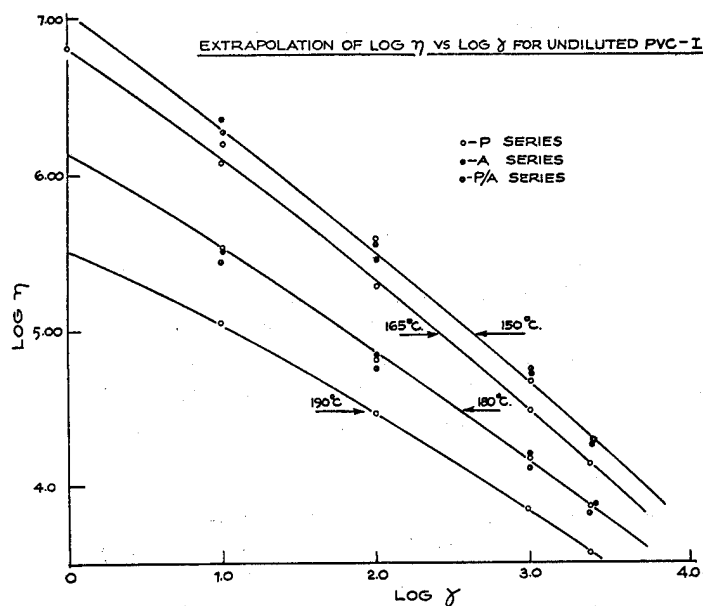


FIGURE 2

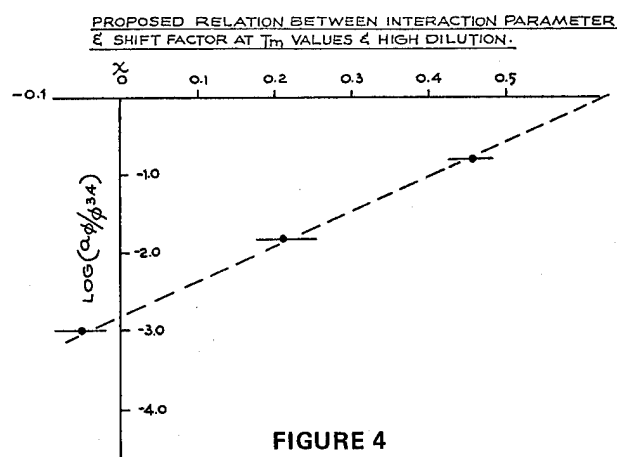


FIGURE 4

## SOME STUDIES OF PROPERTIES OF PLASTICS AT BELL TELEPHONE LABORATORIES

### INTRODUCTION - W. P. Slichter, Director, Chemical Laboratory

Plastics are playing an ever increasing role in the Bell System. In terms of volume, they represent the largest category of materials used in manufacture by Western Electric; before too long they will also represent the largest in terms of tonnage. This commitment comes from the proven merit of modern plastics for a wide variety of applications. However, plastics differ tremendously in type and behavior, so it is important to be both imaginative and wise in their use. Bell Labs., therefore, has long been active in exploring the properties and behavior of plastics, with special attention to understanding these materials so well that we can be confident of their performance. This has to be a continuing process, for plastics technology is growing rapidly and the Bell System's needs are expanding.

The following articles give brief descriptions of some of the work at Bell Laboratories on the nature and properties of plastics in use by the Bell System. This collection is a review of only a fraction of the studies that have recently been in progress. However, they give examples of some modern methods of investigation and of the scope of activities in the field of plastics. Above all, these accounts show the power of fundamental studies to help in the practical use of materials.

### I. ASPECTS OF RELATIONSHIP BETWEEN STRUCTURE AND PROPERTIES OF PLASTICS

S. Matsuoka and T. W. Huseby

There are two immediate goals for those who are conducting applied research in polymer physics or chemistry. The first is to understand the complex behavior of polymers in terms of structural variables, and the second is to apply the knowledge and the results of these studies to practical problems. Our applied research projects are almost invariably long range fundamental investigations, but the topics are often closely related, at least we hope, to important engineering problems within the Bell System.

Many plastics crystallize when they are cooled from the molten state. Unlike inorganic crystals that we are familiar with, polymer crystals attain all levels of degrees of crystallinity depending upon the kind of molecules from which they are constructed (the molecular structure) and the way they are solidified (the processing condition). Studies on the process of crystallization are meant to yield information concerning the properties of the semi-crystalline plastics resulting from various crystallization conditions. Crystals of almost any substances

expand during the melting process. (Water is one of the few exceptions.) The crystallization process can thus be precisely traced by following the time dependence of the volume shrinkage starting from the liquid state (the melt) and ending in the crystalline or partially crystalline state. Figure I-1 represents experimental results from studies on the rate of crystallization of polyethylene. First the sample is melted, then is transferred to the bath at a specified temperature. The sample is small and thermally equilibrates in a matter of seconds, but the subsequent crystallization process proceeds with varying speed depending upon the temperature at which this bath is kept. It can be seen that this process is very sensitive to temperature. For example, it takes about 10,000 minutes or 7 days for this polyethylene to crystallize at 130°C, whereas crystallization is essentially over within 10 minutes at 120°C.

The results from crystallization studies can be utilized in problems concerning the molding or other fabrication processes. For example, the data of Figure I-1 were directly utilized to calculate the relationship between the "half-time" for solidification of polyethylene during injection molding and the temperature of plastics for various injection pressures and cooling rates, as shown in Figure I-2. These results have been found to be useful in designing or improving a mold cycle that would yield a property of the product that is suitable for a specific use.

Figure I-3 is another example of basic data. The frequency-dependent Young's modulus is plotted for high density polyethylene at various temperatures. For example, by studying how these time dependent mechanical properties depend on temperature, one reaches a better understanding of an influence that the structural variables such as the mass fraction of crystals or the texture of the crystalline domains might have on the over-all properties of the polymeric solid.

The data shown in Figure I-3 have also been used in applied problems. Figure I-4 is one such example. The data were utilized to calculate the maximum stress expected in a submarine cable seal. The fact that the mechanical properties are time-dependent makes it necessary to take into account a factor such as the rate of descent into the ocean (which determines the rate of applying the stress in the plastics due to increasing pressure as cable is lowered in the ocean) as well as the temperature and pressure.

## II. DIMENSIONAL STABILITY AND CREEP IN GLASSY POLYMERS

R. S. Moore

In considering the dimensional stability of a plastics for long-term use, consideration should also be given to two factors involving creep of the material. The first involves use of proper molding conditions in order to minimize recoverable strain in the molded product since appreciable recovery would cause shrinkage and/or distortion. These strains are produced by stresses present during molding, and if recovery is not completed at, or near, the molding temperature an appreciable portion of the strain will remain "frozen in". While the material may undergo creep at a slow rate at low temperatures with little or no

immediate adverse effect, in-service use at relatively high temperatures could lead to fairly rapid recovery and distortion. The latter has been observed in at least one instance in a telephone handset wall terminal block in which a high ambient temperature led to appreciable strain recovery and severe distortion. Elevated operating temperatures will probably occur with increasing frequency in future applications as the size and spacing of components become reduced due to miniaturization of parts. Thus, recoverable strain is likely to increase in importance in design considerations.

Quite apart from this is the problem of creep under an imposed load, which occurs even in the absence of recoverable strains. This is of extreme importance in cases in which relatively high temperatures, long times, and often high stresses are involved, as in certain components of standard and ESS miniature relays.

In studying tensile creep (or deformation under a constant tensile force) in a noncrystalline polymeric material when the material is in the so-called rubbery state, the analysis is fairly straightforward. A time scale of the order of 10 or 15 logarithmic decades can often be achieved by making measurements over a few decades in time at different temperatures, and employing a sort of principle of material corresponding states. When this procedure is valid, experiments at higher temperatures provide information on the equivalent material response at longer times and lower temperatures. Provided strains are fairly small, response is almost always found to be independent of stress, i.e., the strain divided by the stress (defined as the creep compliance) is not itself a function of stress.

Unfortunately, neither of the above assumptions is usually valid for glassy amorphous polymers. While the use of measurements at different temperatures to predict equivalent material response at different times may work over a limited time scale in this region, the total response of the material will not be susceptible to such an analysis. This is due in part to the presence of molecular motions with widely different energy requirements. Thus, temperature becomes an additional variable in the study of creep in glassy polymers.

In the glassy response region the creep compliance becomes a sensitive function of stress, even for relatively small deformations. This arises in part because the level of stress required to produce an appreciable velocity of creep is fairly high. It also arises because the energy necessary for material flow is much greater than the available thermal energy. Both of these factors lead to the result that the stress applied to a glassy polymer by virtue of doing work on it, adds the necessary energy and enables the material to undergo displacement to a new position. The results experimentally are often quite dramatic. In poly(methyl methacrylate) an increase in stress by a factor of 10 to a stress level of  $4 \times 10^3$  psi results in an increase in the velocity of creep at room temperature by a factor of 500! Thus, the level of stress is of extreme importance and becomes another variable to be considered in the study of creep in glassy polymers.

Partly because of these considerations, studies of creep in acrylonitrile-butadiene-styrene (ABS) polymers have been undertaken at a series of temperatures at which the acrylonitrile-styrene matrix exhibits glassy response. From studies on Cyclocac T-1000, one of the major ABS polymers used in telephones, it is clear that both temperature and stress must be considered as additional variables in the creep of this material, as well. As an example of the latter, an increase in stress by a factor of 3 results in an increase in creep velocity by a factor of 20 for this polymer at  $60^\circ\text{C}$ , even at relatively short times after loading. In addition, it appears that the temperature dependence of the compliance at short

times is reduced by application of a sufficiently high stress. This also probably occurs because of the energy supplied via the applied stress.

To the influence of these variables on creep response must be added that due to the presence of additives of high and/or low molecular weight, as well as that due to any glass fiber reinforcing materials present. The presence of crystallinity and the nature of the crystalline structure will also influence creep behavior as will effects of humidity on hygroscopic materials. Such effects add to the already complicated response in creep but it is believed that investigations of such materials can provide insight into the nature of their influence. That these materials are of interest is clearly seen in the use of glass-filled nylon relay components containing  $\text{MoS}_2$  and teflon.

## HIGH SPEED TESTING

One of the major problems in considering impact properties of materials is the detection of material deformation and response at high strain rates or at high rates of loading. The problem of merely detecting changes in sample shape via high speed photography poses a rather difficult task, so that relatively few data are available. Detection of contours of stress concentration through photoelastic techniques is likewise rather difficult and the simpler problem of measuring changes in birefringence (changes in refractive index parallel and perpendicular to the direction of tensile stress) is considered the more desirable experiment for initial investigations. This experiment still allows one to obtain information on molecular orientation occurring during deformation even though the detailed distribution of stresses is not obtained. Both this area and that using high speed photography are being investigated as to applicability to testing at rates up to 8700 inches per minute. It is anticipated that up to 12 photographs of 1 to 3 microseconds exposure can be obtained at intervals up to a few milliseconds. Use of transparent materials provides a distinct advantage and great simplification to the experimental set-up since the study of opaque polymers requires the bonding of photoelastic materials to the substance under investigation. Techniques using holography in the detection of small deformations in opaque materials have also been considered and information on their application is also available.

## III. DYNAMIC MECHANICAL PROPERTIES OF PLASTICS

J. H. Daane

In this section we present a brief description of dynamic mechanical testing and then illustrate, with an example, its usefulness in understanding macroscopic mechanical properties in terms of polymer microstructure. Dynamic mechanical tests measure the response of a material to periodic forces, usually sinusoidal in nature. A perfectly elastic body will respond in-phase, i.e., the potential energy stored in the body will be completely recoverable. Polymers are not perfectly elastic, however, and possess an out-of-phase component which dissipates energy as heat. The ratio between the energy dissipated per cycle to the maximum energy stored per cycle is termed the loss tangent. This quantity may be determined directly on several commercially available instruments. Another quantity obtainable is modulus or the slope of the initial straight line portion of a stress-strain curve. From a knowledge of the specimen dimensions and the dynamic

force and loss tangent determined on the instrument, we may calculate a dynamic modulus of elasticity, i.e., the in-phase modulus and also an out-of-phase or loss modulus.

In conducting these tests, either frequency or temperature of testing may be varied while holding the other constant. We find it usually convenient to vary temperature. Observation of the loss tangent or loss modulus as temperature is varied will reveal, in the case of polymers, a loss maximum when the predominant or characteristic relaxation time of the polymer equals that of the reciprocal of the test frequency. In other words, the characteristic relaxation time of the polymer changes with temperature and will result in a loss maximum when it matches that of the test cycle. This maximum in loss occurs, for example, when a polymer changes from the glassy state to the rubbery state. This temperature is called the glass transition temperature.

Figure III-1 illustrates the case for a composite material, ABS, which is an interpolymer of styrene-acrylonitrile copolymer grafted onto butadiene rubber particles. ABS is the material currently used in telephone handsets. Loss moduli of a series of varying compositions are plotted versus temperature of testing at 138 cps. The occurrence of two loss peaks, appearing at the characteristic relaxation times of the two respective components, indicates that each component is present as a discrete phase. If the material were mechanically homogeneous, only one broad loss peak would be expected to occur somewhere between the glass transition temperatures of the two components. Note the drop in the in-phase modulus as the butadiene rubber component changes from the glassy state into the rubbery state. Figure III-2, an electron micrograph of an ABS fracture surface broken at liquid nitrogen temperature, verifies the existence of separate phases. The spheroidal rubber (butadiene) particles, which range in size from 0.1 to 1.5 microns in diameter, are sufficiently large that both the butadiene rubber and the SAN components retain their inherent mechanical properties. Thus the dynamic mechanical properties of the interpolymer reveal the microstructure of this material.

Figure III-3 illustrates room temperature, low speed, stress-strain behavior of the SAN by itself and then after modification with the butadiene. The butadiene was added to improve the material's ability to absorb and dissipate energy which is represented by the area under the respective stress-strain curves. The large increase in area in going to the composite can be seen to result from the enhancing of the ability of the composite to yield and draw to high elongations before ultimate failure. Thus, the normally brittle matrix is induced, by the incorporation of the butadiene particles in the proper size and manner, to absorb much more energy before failure. That the glassy matrix does indeed yield and draw on a local scale is illustrated in Figure III-4. This is another electron micrograph of an ABS fracture surface broken in the vicinity of the butadiene glass transition temperature.

Results from high speed tensile tests (10,000 in/min), carried out over a large temperature range, are summarized in Figure III-5. An oscilloscope was used to record force-elongation curves whose areas were then measured and plotted versus the temperature of testing at constant cross-head speed. The upper line represents total area of the curves while the lower represents the area only up to the yield point. The total area is seen to increase with temperature while the area to yield remains essentially constant. Note that the two lines appear to converge in the vicinity of the butadiene glass transition temperature. Below this temperature the material would not yield and would fail brittly as it does normally at room temperature without the butadiene present.

In summary, we have seen that a material (SAN), normally brittle up to its own glass transition temperature of  $100^{\circ}\text{C}$ , has been transformed into one that yields and draws down to the vicinity of the glass transition temperature of the added butadiene component. The interpretation of this macroscopic mechanical behavior in terms of microscopic deformation has been possible through the use of dynamic mechanical tests.

#### IV. THERMAL ANALYSIS OF PLASTICS

H. E. Bair

During the past few years, modern electronic technology has been utilized successfully to develop instruments which are capable of detecting minute changes in the heat content of a system undergoing a chemical or physical process. These new calorimeters permit the determination of many thermodynamic properties of plastics which could not be measured on other types of differential thermal analyzers. The purpose of this paper is to report some calorimetric information which has been obtained on semi-crystalline and glassy plastics in our laboratory. The selected thermal studies which are shown here range from the determination of the degree of crystallinity of polyethylene to the quantitative analysis of the components of a blend of plastics.

Figure IV-1 shows the response of the calorimeter at a heating rate of  $10^{\circ}\text{C}/\text{min}$ . to the melting of polyethylene crystals which had been grown in solution at  $85^{\circ}\text{C}$ . It should be noted in this figure that the temperature is displayed along one axis and the amount of heat gained or liberated per unit time by the sample is represented along the axis which is perpendicular to the temperature scale. The latter quantity is proportional to the specific heat of the material, which is the amount of heat (usually expressed in calories) necessary to raise the temperature one degree centigrade per gram of material.

The apparent specific heat of the crystals rises sharply during the transformation of the solid crystals into a liquid or melt with almost ninety per cent of the crystals melting between  $124^{\circ}\text{C}$  and  $127^{\circ}\text{C}$ . In this special case, the highest observed melting temperature of the thin lamellae may be used to calculate the thickness of the crystal. X-ray measurements have indicated a lamellar thickness of  $126 \text{ \AA}$ . In addition, it may be concluded from the narrowness of the melting curve that most of the crystals have the same dimensions. From the area under the curve the latent heat of fusion or total amount of heat which was absorbed in order to melt all the crystals in this sample may be determined. In this case, 57 calories per gram ( $\text{cal/g}$ ) were gained during fusion. Independent measurements have shown that 68  $\text{cal/g}$  would be required to melt a completely crystalline sample of polyethylene. Thus, the apparent degree of crystallinity of this particular sample is equal to the ratio of 57 to 68 or 0.84. Thus, the shape of the melting curve may give valuable information about the structure of polymer crystals.

Recently, a problem arose concerning the structural identity of the material being used to make cables. It was not known whether the material in use was the intended copolymer of polyethylene and butene or by mistake was a linear homopolymer of polyethylene. The problem was solved by making a thermal fingerprint

of the unknown material and comparing it with the melting behavior of materials whose molecular structures were known.

Nearly identical weights of linear polyethylene (Marlex 6002, Natural), a copolymer of polyethylene and butene (Marlex 5003 and 0.75% butene, Natural), a copolymer of polyethylene and butene with carbon black (this copolymer, Phillips P6402021, has the same molecular structure as the previous copolymer) and the unknown were melted to remove all previous thermal history. Then the samples were cooled from the melt at 100°C/min. to 30°C. The subsequent melting of each sample is shown in Figure IV-2.

The linear homopolymer is more crystalline and has a final melting temperature 10°C above the copolymer. As expected, the melting behavior of the natural and black copolymer are identical except for the slightly smaller amount of heat absorbed by the carbon filled material. The similarity of the melting curves of the unknown plastics and the copolymer indicates that the material in question is a copolymer and not linear polyethylene.

There are presently many blends of plastics on the market. Unfortunately, many manufacturers will not reveal the phase content of these blends. Therefore, it is often necessary to determine ourselves the components which make up a blend and the amounts of each material in a blend. A thermal analytical technique is one convenient method for this purpose.

At a particular temperature, which is dependent upon the molecular structure of the plastics and the heating rate of the experiment, the thermal response of a glassy plastics will change to liquid-like behavior. This temperature is called the glass transition temperature,  $T_g$ , and it is characterized thermally by an increase in the level of specific heat of the material. In principle, the type and amount of a plastics and a blend may be found by measuring the glass transition temperature and the magnitude of the increase in specific heat which occurs at this temperature.

In Figure IV-3 the thermal response of two glassy resins is shown. Resin I is a copolymer of PVC and propylene with a small amount of "impact modifier" added. At approximately 80°C the transformation of the glassy PVC to liquid PVC occurs. The size of the change in specific heat at this temperature is about 95% of the magnitude of the change for pure PVC. A small transition occurs at about 120°C which is probably due to the impact modifier which constitutes the remaining 5% of the material. The transition temperature of the impact modifier suggests that it is probably an ABS type resin.

Resin II (Figure IV-3) exhibits three separate glass transitions. This indicates that the blend is composed of three separate phases: a rubber (polybutadiene) component ( $T_g = -75^\circ\text{C}$ ), a PVC component ( $T_g = 81^\circ\text{C}$ ) and polystyrene-acrylonitrile (SAN) copolymer ( $T_g = 107^\circ\text{C}$ ). From the magnitude of the specific heat changes accompanying these transformations it may be concluded that the blend is composed of 4 or 5% rubber, 46% PVC, and about 45% SAN. From the thermal behavior of the rubber it may be inferred that about 50% of the SAN is free and the remainder is part of the ABS material.

## V. ASPECTS OF ADHESIVE JOINTS

T. K. Kwei

During the last few years, we have been interested in the load-bearing ability of adhesive joints in a humid environment at moderately high temperatures. Many adhesives are sensitive to moisture, and, in the wet condition, the strength may decrease markedly, sometimes to less than half the strength in the dry state. Usually the data used for design purposes are obtained at room temperature by a short-term strength test and the results may not reflect a complete picture of the permanence of an adhesive joint under constant load in a humid environment.

Since the stress distribution in an adhesion joint is very complex, we have approached the problem, as a first step, by studying the load-bearing ability of the adhesive itself in a humid atmosphere. It is well known that if a load somewhat less than the ultimate strength of a material is applied to a sample, the sample will eventually break, after a period of time, under this stress. Experimentally, we measure the time to break,  $t_b$ , at a given load under a variety of temperature and humidity conditions. Typical results for an epoxy polymer are shown in Figure V-1.

At each temperature there is a lower limit of stress shown as a dotted line, below which the breaking time exceeds 500 hours when the experiment is terminated. The epoxy polymer used in this study has a glass transition temperature of about 52°C. It can be seen from the figure that a dry polymer is able to sustain a much higher stress over a long period of time at temperatures below the glass transition. As temperature increases the strength decreases and the breaking time becomes very short. In the presence of 100% relative humidity the load-bearing capacity of the polymer decreases substantially even at low temperatures, and the polymer behaves almost like a different material. When similar epoxy polymers having higher glass temperatures (anhydride cured, for example) are tested in a similar manner, the effect of humidity is less pronounced at low temperatures. Our data also suggest that if an epoxy adhesive with a low glass temperature is used, the moisture sensitivity may become very serious. This is indeed the case with adhesive joints using polyamide-polyamine epoxies and nylon-epoxies.

An analysis of our results, according to current theories, leads to the conclusion that absorbed water molecules act effectively as plasticizers. In order to understand the phenomenon better, we are in the process of setting up an apparatus to measure the rate and maximum amount of water absorption. An attempt to relate these measurements to mechanical properties will be carried out. In addition, a study of the effect of various curing agents and curing conditions is in progress.

## VI. SOME ASPECTS OF THE FLOW BEHAVIOR OF POLYMER MELTS RELATED TO PROCESSING

L. L. Blyler, Jr.

## INTRODUCTION

The flow behavior of polymer melts is very different from that of more conventional liquids and a number of examples of unusual behavior can be cited:

1. Polymer melts are non-Newtonian. Newtonian fluids have constant viscosity at any given temperature and pressure. The viscosity of a polymer melt also depends upon the rate at which it is sheared. A typical plot of viscosity against shear rate (velocity gradient) for a high density polyethylene melt obtained from capillary extrusion rheometer measurements is shown in Figure VI-1. It may be seen that a 100-fold increase in shear rate results in a 10-fold decrease in viscosity.
2. When a polymer melt is extruded through a die, the emerging extrudate is observed to swell, so that the diameter of the extrudate is larger than the diameter of the die itself.
3. If a polymer melt is extruded through a die at increasing rates, a point is reached at which the surface of the extrudate begins to take on a rough appearance. As the rate is increased further, the roughness becomes more pronounced. This flow instability has been called "melt fracture".
4. Experiments involving injection of dye traces into polymeric fluids flowing through tubes show clearly that these fluids recoil upon sudden stoppage of steady flow and, therefore, possess a recoverable strain.

All of the aforementioned phenomena can be explained at least qualitatively by postulating that flowing polymer melts simultaneously possess both viscous and elastic properties. This is a reasonable conclusion when one considers that a polymer melt consists of a collection of long chain molecules, existing in a randomly coiled condition when the melt is at rest. If the molecules are long enough, they can become entangled and intertwined with one another, as depicted in Figure VI-2. The longer the molecules are, the greater the number of entanglements in which each one can participate. Therefore, it is to be expected that the properties of polymer melts will depend very strongly on such factors as molecular weight, molecular weight distribution, and whether or not long branch chains are present on the main molecular chain.

This mass of polymer molecules comprising a polymer melt may be considered to form a network in which the points of entanglement are the network junctions, also depicted in Figure VI-2. Of course, these junctions are not permanent because the entanglements can slip. The links between the network junctions consist of randomly-coiled segments of the polymer chains.

If the polymer melt is made to flow by imposing an external stress, the network will respond in two ways:

1. The molecular segments connecting entanglement points uncoil and orient, resisting the deformation because a random configuration is preferred; this mechanism gives rise to elasticity, and is characterized by a modulus and an elastic strain.
2. The molecules can disentangle and slip past one another into a new

configuration; this mechanism gives rise to flow and is characterized by a viscosity.

When a polymer melt undergoes flow, both the viscous and elastic mechanism occur simultaneously. Consequently, when dealing with processing applications, elastic behavior, as well as viscous behavior, must be considered. For example, extrusion processes must be designed to accommodate extrudate swelling, "melt fracture" imposes an upper limit on extrusion speed, and care must be exercised to avoid freezing large elastic strains generated in the flowing melts into fabricated parts as residual strains, which might later lead to failure or lack of dimensional stability.

## VISCOUS BEHAVIOR

Melt Index\* is a widely used parameter for characterizing the viscous behavior of polymer melts. However, it represents only a single point on the viscosity curve of a polymer melt and difficulties may arise if melt index is used as the sole criterion of processability.

To illustrate this point, Figure VI-3 depicts the flow curves (log shear stress against log shear rate) of two polymer melts at 190°C and 225°C, obtained with a capillary extrusion rheometer. Polymer A is a copolymer of ethylene and acrylic acid containing 15% by weight acrylic acid. Polymer B is a high density polyethylene. Both materials have a melt index of 5.

The 190°C flow curves for Polymers A and B converge at low shear stresses. This behavior reflects the equivalence of the melt indices of the two materials, since melt index is a low shear stress parameter. At higher stresses, however, the curves diverge widely. At a shear rate of 1000 sec.<sup>-1</sup> Polymer A is nearly three times more viscous than B, and, therefore, would be a great deal more difficult to process.

A 35°C increase in temperature produces a much greater shift in the flow curve for Polymer A than for Polymer B. The extreme temperature sensitivity of viscosity exhibited by Polymer A results in a decrease in the disparity between the flow curves at 225°C. At 1000 sec.<sup>-1</sup> Polymer A now has only twice the viscosity of B. Consequently, increasing temperature leads to greater relative gains in processability for Polymer A than for Polymer B.

Another important implication of the flow curves in Figure VI-3 bears on the problem of discoloration and "burning" of injection molded parts. In the injection molding machine there exist regions of high local shear. Since polymer melts are highly viscous, a great amount of energy dissipation occurs in these regions and the local temperature rises to levels at which degradation is extremely rapid. Because viscous energy dissipation is directly proportional to viscosity, the 190°C flow curves in Figure VI-3 indicate that at 1000 sec.<sup>-1</sup> Polymer A dissipates into heat three times more energy than Polymer B. Consequently, much larger local temperature rises will occur with Polymer A and degradation is a definite possibility.

Summarizing, the details of the flow curves of polymer melts can have important implications for processing which are not at all evident from simple index measurements.

\*Melt index is defined as the weight in grams of polymer melt extruded from a standard reservoir at 190°C under a load of 2160 grams through a capillary of specified dimensions during a 10-minute interval.

## ELASTIC BEHAVIOR

One of the important consequences of the elasticity exhibited by flowing polymer melts is that elastic strains can be frozen into fabricated parts. This situation is usually to be avoided since residual strains often lead to failure of parts. In order to approach this general problem in a systematic way, it is necessary to obtain measurements of the recoverable elastic strain in flowing polymer melts as a function of rate of shearing and temperature, and to understand how the strain depends upon the molecular structure of the polymer. Unfortunately, the recoverable strain is a rather difficult quantity to determine accurately. Some of the methods which have been employed to measure it are listed below:

1. Measurement of recoil upon sudden stoppage of steady flow. This method is direct but rather inaccurate.
2. Flow birefringence measurements. This method is very precise but requires highly specialized equipment.
3. Measurement of tensile normal stresses. Owing to their elasticity, polymer melts are capable of supporting a tensile stress; in fact, shearing a polymer melt induces the formation of tensile stresses. Equations resulting from a number of theories exist which relate these tensile stresses to the recoverable strain. Tensile normal stresses can be measured with the Weissenberg rheogoniometer and with a capillary rheometer by determining capillary end corrections.
4. Dynamic modulus measurements. The use of correlations which exist in theory between the dynamic (oscillatory) behavior and steady flow properties enables the calculation of recoverable strain from dynamic shear modulus measurements.

Some preliminary measurements of recoverable strain carried out using the latter two methods are shown in Figure VI-4. This graph shows the recoverable strain,  $S_R$ , as a function of shear rate for two high density polyethylene melts. Large discrepancies between the curves obtained by different methods are evident. The dynamic modulus method gives values for  $S_R$  which are ridiculously high, while the tensile shear method yields much more reasonable values. Further work is being carried out to resolve the discrepancies so that a meaningful approach to the residual strain problem can be made.

The flow behavior of polymer melts is extremely complex owing to their complicated molecular structure. Consequently, it is frequently necessary to understand the details of this behavior in order to carry out processing operations intelligently.

## VII. APPLICATION OF GEL PERMEATION CHROMATOGRAPHY TO MOLECULAR WEIGHT POLYDISPERSITY IN POLYMERS

R. Salovey

Until a few years ago the determination of the molecular weight distribution

of a polymer was, at best, a tedious process. It involves dividing the polymer sample into cuts or fractions, each of which was rather homogeneous, and determining an absolute molecular weight for each fraction. Knowing the weight of each cut we reconstruct the molecular weight distribution.

Table VII-1 illustrates the fractionation of polyethylene which has been packed into a column and eluted (extracted) with mixtures of increasing solvent power. The fractions come off the column in order of increasing molecular weight. The fractions were characterized by measuring the intrinsic viscosity - which is a measure of the capacity of a polymer molecule to enhance the viscosity (or rate of flow in a capillary tube) of a solvent and is related to the molecular weight. The number average molecular weight was determined by membrane osmometry. The column labeled elution volume refers to the new technique of gel permeation chromatography. This fractionates in inverse order from the column fractionation. The advent of commercial gel permeation chromatographic equipment has revolutionized measurements of molecular weight distribution for the polymer chemist. In gel permeation chromatography, polymer molecules are separated by their ability to permeate, or pass through, a porous gel. High molecular weight components cannot penetrate the gel network and elute first. The elution volume refers to the volume of solvent necessary to carry the polymer to a detector at the end of the column. Molecules of decreasing molecular weight find more available volume in the gel, that is, penetrate further into the gel, and require more solvent to elute. Thus, the elution volume in gel permeation increases with decreasing molecular weight. With suitable detection, gel permeation chromatography is a simple method of fractionating a polymer into component molecular weights.

Figure VII-1 is an experimental chromatogram. Polymer emerging from the column at different elution volumes is detected by measuring changes in refractive index, which are proportional to concentration. In order to interpret such a curve in terms of molecular weight, it is necessary to calibrate the elution volume. Fractions of the polymer type considered may be obtained from a column fractionation and the absolute molecular weight of each fraction is determined. These samples are then injected into a gel permeation chromatograph to yield a sharp peak. The elution volume at the maximum can then be associated with a given molecular weight. Figure VII-2 is a typical calibration curve. Distinct calibration curves are obtained for linear and for branched polyethylene. It is usually found that the logarithm of molecular weight is linear with elution volume. At the high molecular weight end of both curves, the elution volume becomes less sensitive to molecular weight as the very largest molecules do not penetrate the gel, but pass through the column around the spherical gel particles (through the interstitial volume). From a calibration curve and experimental gel permeation chromatograms it is possible to construct a differential distribution curve as shown in Figure VII-3. This is a plot of the weight fraction of molecules of given molecular weights.

TABLE VII-1

FRACTIONATION OF BRANCHED POLYETHYLENE

<u>Fraction</u>	<u>Weight Fraction</u>	<u>Elution Volume</u>	<u><math>\bar{M}_n \times 10^{-3}</math></u>	<u><math>[\eta], \text{dl/g}^a</math></u>
1,2,3	0.0345	119.0 ml	-	-
4	.0348	115.5	-	-
5	.0501	112.5	10	-
6	.0442	109.5	13	0.28
7	.0241	108.0	19	0.51
8	.0697	106.5	22	-
9	.0722	103.5	34	0.95
10	.0772	102.0	37	1.00
11	.1186	100.75	41	-
12	.0688	99.0	53	-
13	.0938	96.5	71	1.45
14	.1165	94.0	160	1.95
15	.0886	93.0	280	2.42
16	.0754	91.5	900	2.90
17	.0315	91.0	-	-

<sup>a</sup>In decalin at 70°C.

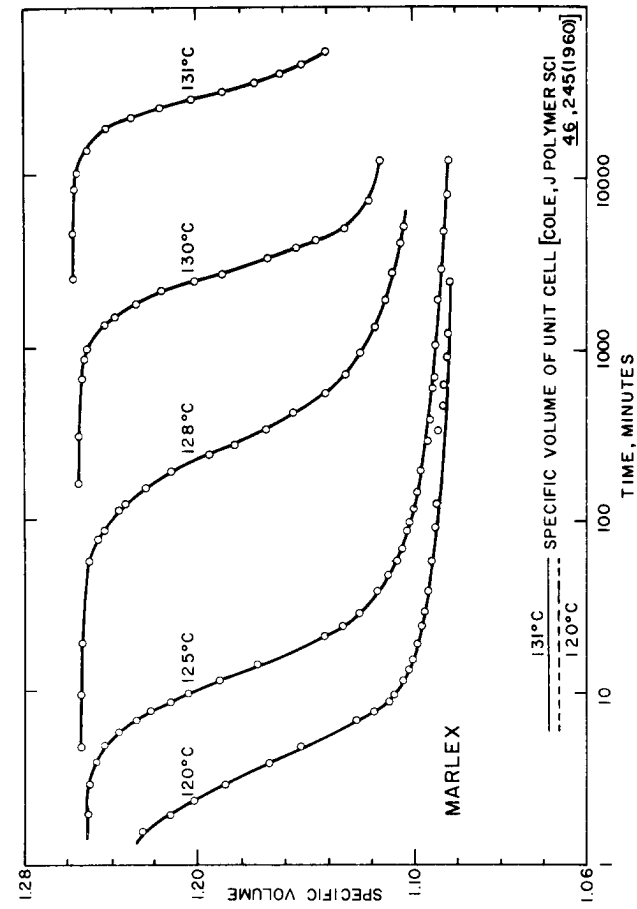


FIGURE I-1

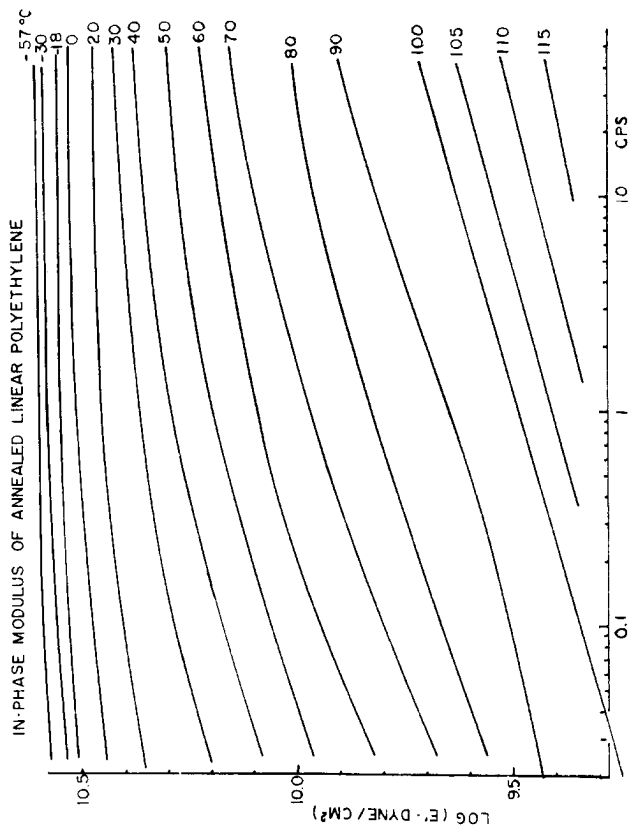


FIGURE I-3

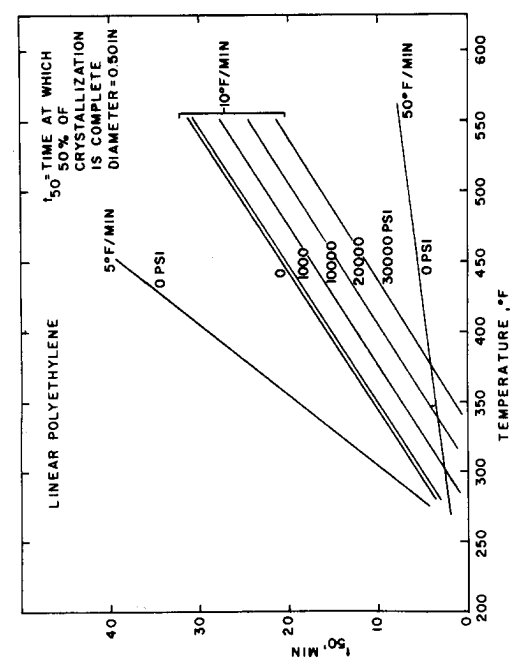


FIGURE I-2

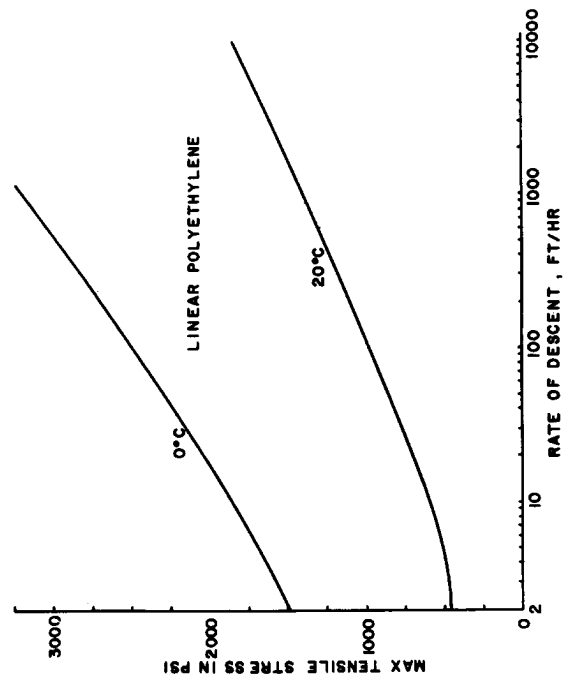


FIGURE I-4

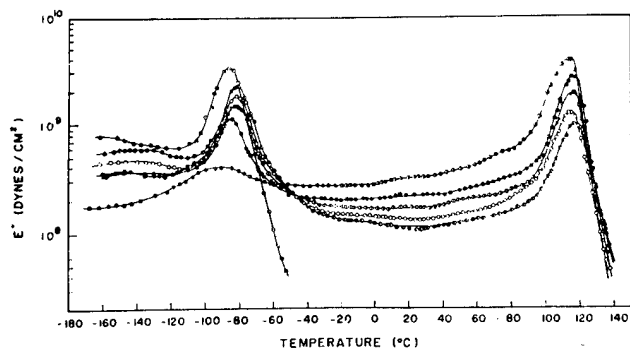
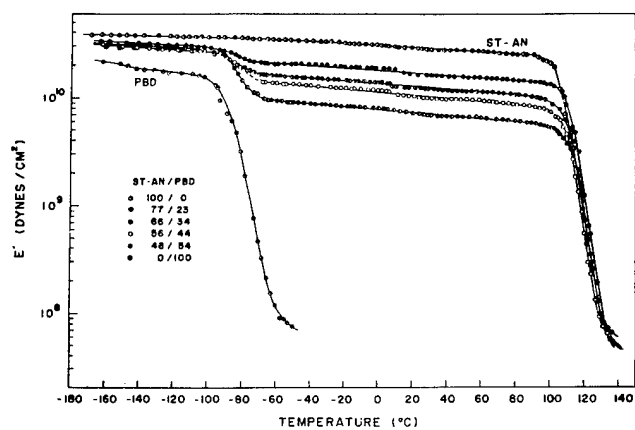


FIGURE III-1



FIGURE III-2

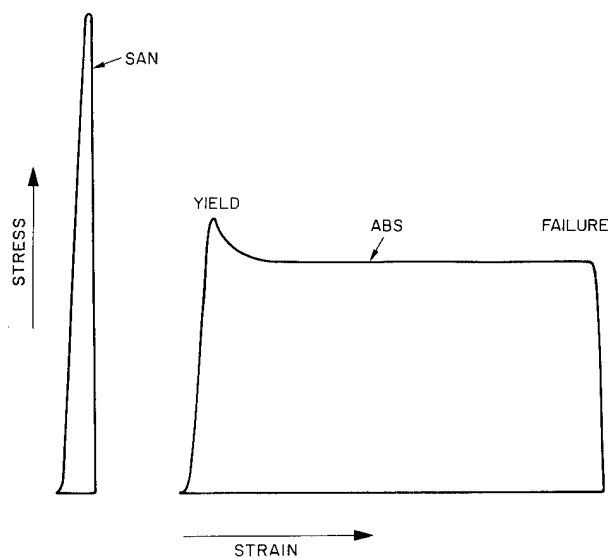


FIGURE III-3

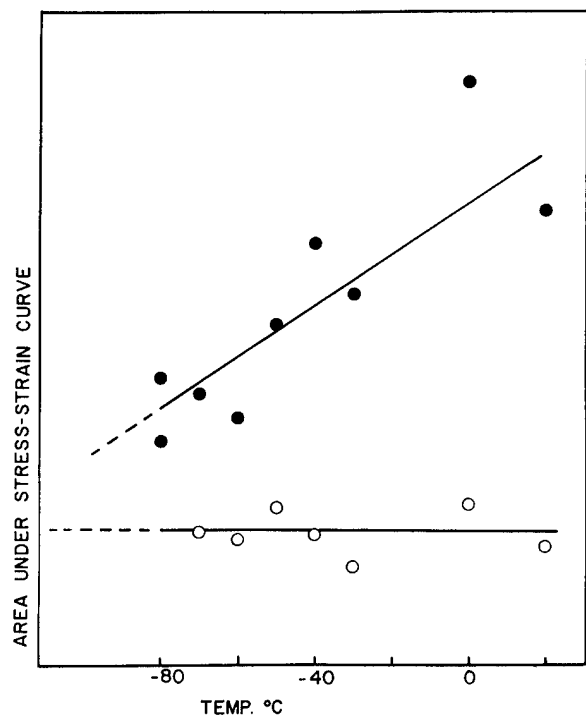


FIGURE III-5



FIGURE III-4

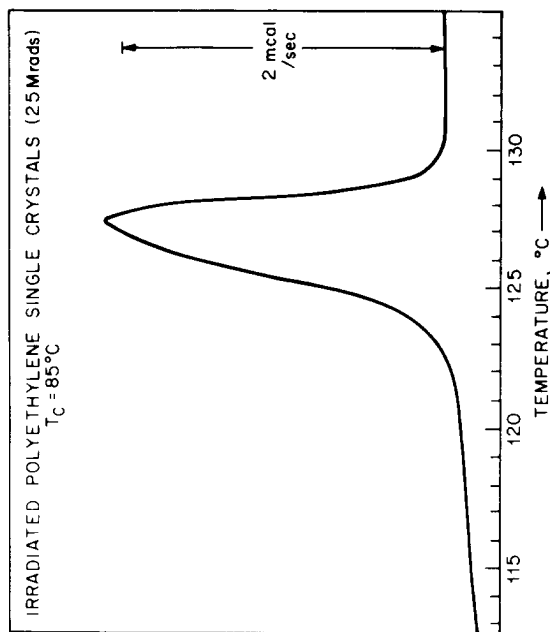


FIGURE IV-1

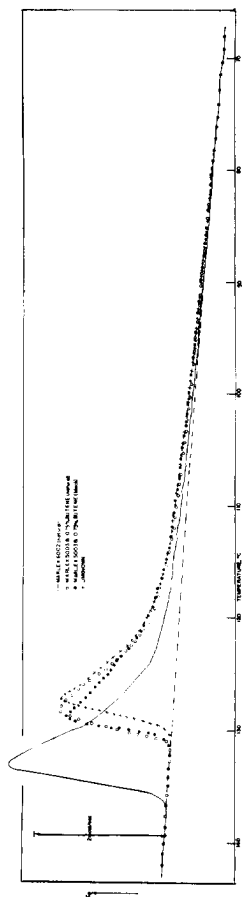


FIGURE IV-2

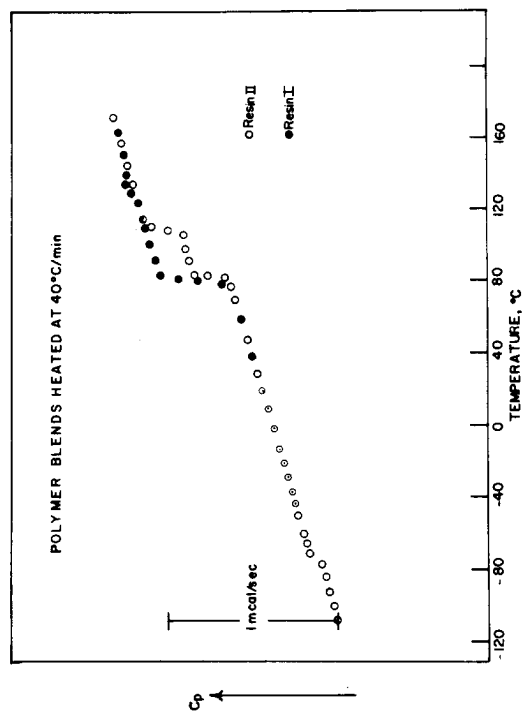


FIGURE IV-3

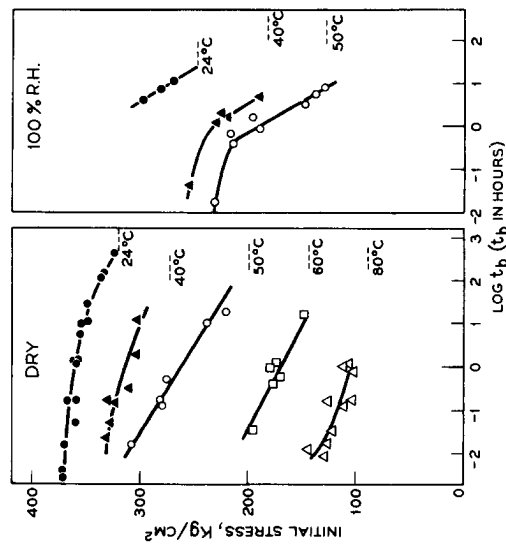


FIGURE V-1

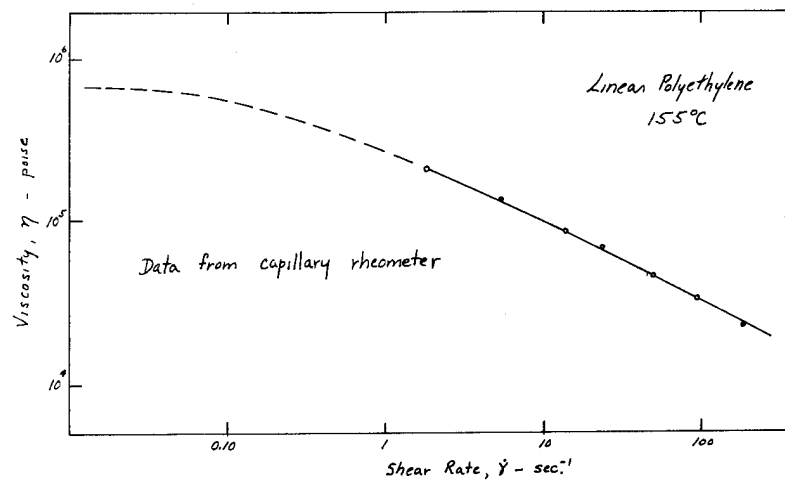
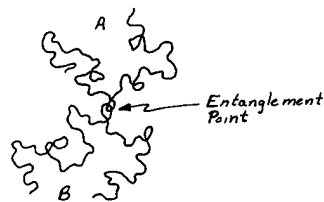


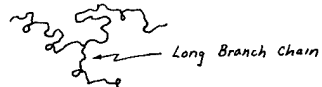
FIGURE VI-1

Molecular Model of Polymer Melt (at rest)

- 1) Collection of randomly coiled long chain molecules
- 2) If molecular weight is high enough, entanglements possible



- 3) Properties will depend strongly on molecular weight, distribution of molecular sizes, degree of long chain branching



- 4) Consider the collection of molecular chains to form a network with entanglement points as (non-permanent) network junctions



FIGURE VI-2

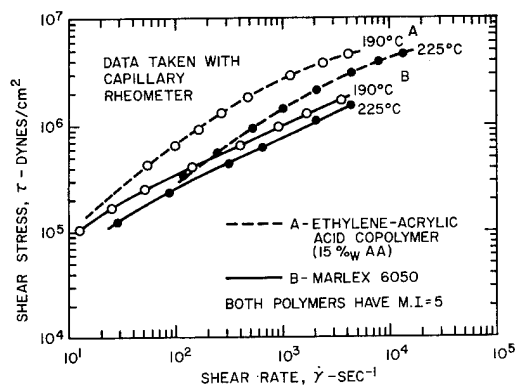


FIGURE VI-3

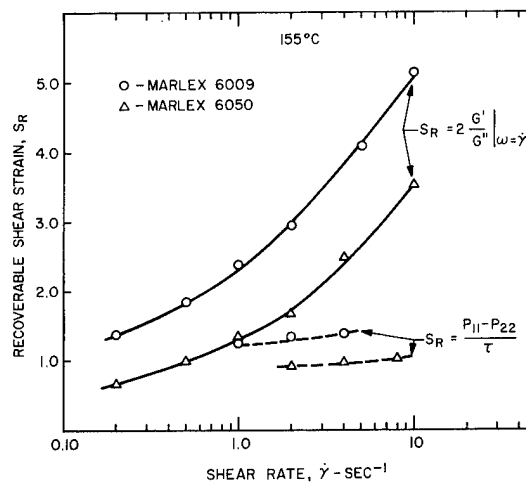


FIGURE VI-4

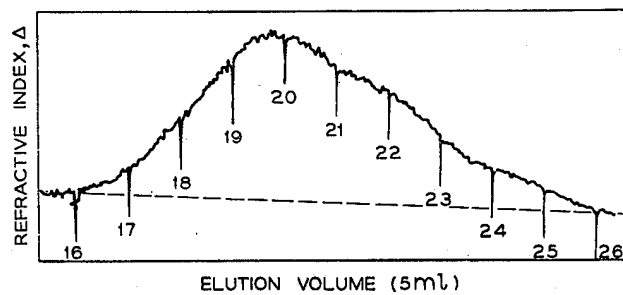


FIGURE VII-1

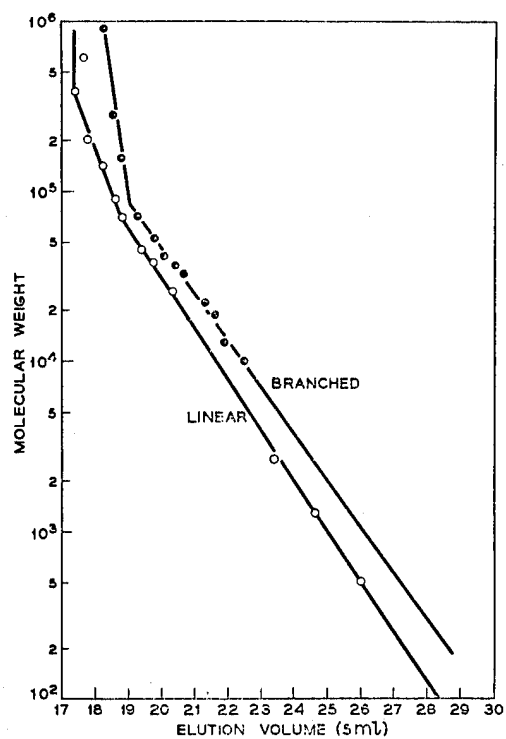


FIGURE VII-2

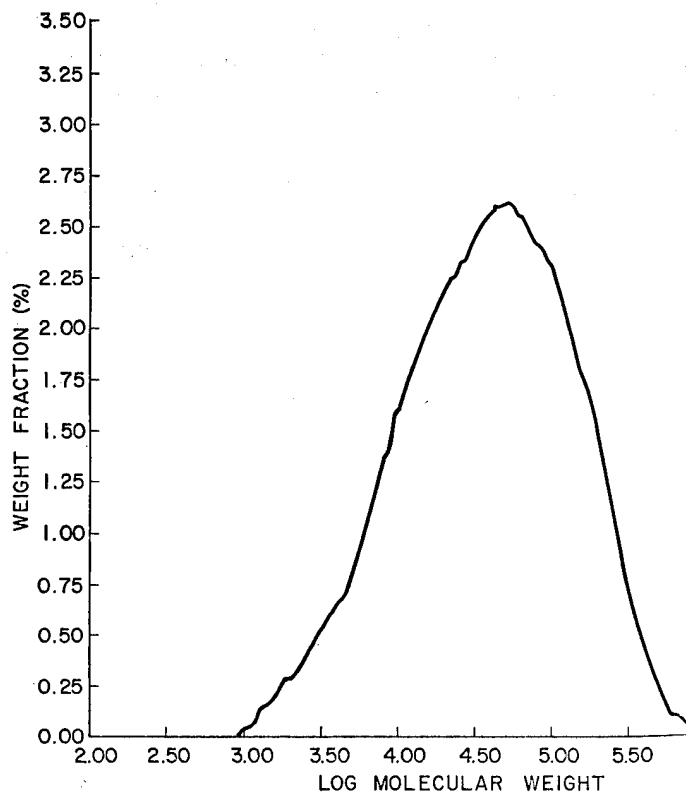


FIGURE VII-3

## ABSTRACT

### NONLINEAR VISCOELASTIC CHARACTERIZATION OF POLYMERIC MATERIALS

R. A. Schapery

School of Aeronautics, Astronautics and Engineering Sciences

Purdue University

Lafayette, Indiana

Nonlinear, viscoelastic response of hard and soft polymers is first reviewed in order to bring out certain common features of their creep (constant stress) and relaxation (constant strain) behavior. It is shown that the time-dependence of nonlinear behavior often can be expressed in terms of the same creep and relaxation functions that define response to small stresses and strains.

When such behavior exists, thermodynamic principles lead to relatively simple, multiaxial stress-strain relations which are valid under constant or varying stresses, strains, and temperature. These equations are very similar to the Boltzmann form in linear viscoelasticity theory. They provide, therefore, direct guidelines for the design of experiments and data analysis needed to characterize polymers for stress analysis purposes.

Using existing data on plastics and elastomers, including a glass fiber-reinforced phenolic, some example applications are made in order to illustrate methods of data reduction and accuracy of the method in predicting response to time-dependent loading.

03

ASPECT OF ULTIMATE PROPERTIES: MECHANICAL FATIGUE

George P. Koo

Plastics Division

Allied Chemical Corp.

Morristown, N. J.

## INTRODUCTION

The inherent toughness of polymeric materials is manifested in two outstanding end-use properties; namely, the resistance to impact and to mechanical fatigue. Perhaps because the importance of impact resistance in pertinent applications is easily visualized and is an unequivocal design consideration, the necessity of impact testing is clear and impact tests have flourished. While current understanding of the phenomenon with respect to polymer structure and composition leaves much to be desired, at least the limitations of popularly used test methods are well known, and fruitful fundamental research via high speed testing and dynamic mechanical techniques are being done.

On the other hand, although numerous applications take advantage of the resistance to repeated loading (e.g., bellows, couplings, and gears), the relationship of the application to a single property, fatigue resistance per se, is complicated and indirect and is not usually obvious. Hence, relatively less work has been done in the field to understand the fatigue behavior of polymers. In areas where specific objectives relative to end use is clear, such as reinforced laminates for aerospace applications, elastomers for tires and monofilaments of potential fibers, much experimental work has been done. However, from the results of investigations so motivated, it is not always possible to separate out the effects inherently due to the polymer.

The purpose of this paper is to illustrate the complications when considering the fatigue behavior of polymers under conditions that simulate some applications, to describe some unusual behavior seemingly specific to polymers, and hopefully to stimulate interest that would result in initiating other investigations.

In order to establish a reference base for the discussion to follow, it is necessary to briefly describe some general aspects of fatigue testing. Except in one very important respect to be discussed, fatigue testing of polymers is similar to the established traditional techniques applied to older engineering materials. The cyclic loading is usually sinusoidal, in either reverse tension, compression, combination of tension and compression, bending or torsion. The peak stress or maximum strain amplitude is held constant as is the test temperature. The data are most frequently presented semilogarithmically as stress (or strain) versus decades of cyclic life to failure - the so-called S-N curves. If an asymptotic stress level is experimentally found below which the material will not fail, the material is said to have an endurance limit at that stress. (Examples for

polytetrafluoroethylene and polychlorotrifluoroethylene are shown in Figure 1.)

Just as metals and alloys have crystalline imperfections and impurities, polymer samples also contain inhomogeneities. If fatigue failure is a function of the very presence of inhomogeneities, then from the purely statistical nature, one can expect a great deal of scatter in the data. This inherent scatter, in spite of careful technique, can be as much as two decades in an S-N plot. Consequently, statistical treatment of the data is a frequent necessity; further discussion of this aspect can be found in an excellent overall summary on fatigue by Richards.<sup>1</sup>

The point of emphasis is that metals for structural uses, heretofore the dominating engineering material, do by and large fail in fatigue catastrophically due to internal inhomogeneities. The basic mechanistic explanation is that stress concentration about an imperfection leads to crack initiation which propagates until catastrophic fracture occurs. Various laws and theories formulated on the nature of fatigue damage and failure are based on this premise, namely, fatigue failure by fracture is dependent upon crack initiation and propagation.

Under properly controlled conditions, crack propagation of polymers under cyclic stress also follow the same behavior. Burns and co-workers<sup>2</sup> conducted some interesting and careful studies of crack propagation of poly(methyl methacrylate) under cyclic loads at low frequency and at room temperature. Random crack initiation was obviated by prenotching large, flat PMMA sheets and following the crack growth under reverse tensile load. Their data showed that under those conditions, crack growth is quite similar to metals. As shown by Equation (1), a simple relationship describes the crack growth rate

$$\frac{da}{dN} = C (\Delta K)^m \quad (1)$$

where  $a$  = crack length  
 $N$  = number of cycles  
 $\Delta K$  = stress intensity factor which is a function of stress, crack length and geometry of the specimen  
 $C, m$  = constants derived from the data

However, above results are taken with temperature held constant. Under conditions where polymers are viscoelastic, significant heating may arise continuously, changing the temperature of the test specimen. Experimental results from such complications do not and cannot follow analysis where temperature is assumed constant. A recent review<sup>3</sup> makes the specific point that the damage that results from fatigue testing is of two non-mutually exclusive but distinct natures. One stems from the strong time dependent nature of polymers, and the second is effects directly attributable to some form of crack growth such as the work of Burns, et al.<sup>2</sup>

The condition of some of current and future cyclic loading applications of plastics may be such that the extent of heating actually controls performance. Therefore, it is important to consider the effects of hysteretic heating of a polymer during cyclic loading, and is the central theme of the remainder of this paper.

# ANALYSIS OF LINEAR VISCOELASTIC MODEL

First, it is instructive to consider a linear viscoelastic model under dynamic loading. The ensuing discussion modified from Vincent<sup>4</sup> is worth repeating by virtue of its simplicity and clarity.

Let us suppose that stress is the sinusoidal forcing function as represented by

$$\tau(t) = \tau_0 \sin \omega t \quad (2)$$

and is equivalently shown as a rotating vector on a stress-time diagram (Figure 2a). By definition, the strain of a linear viscoelastic material lags behind the stress by a constant phase angle,  $\delta$ . As shown by Figure 2b, strain can be represented by

$$\epsilon(t) = \epsilon_0 \sin (\omega t - \delta) \quad (3)$$

It is obvious from the diagram that the stress vector can also be considered to be the sum of two separate components; one of which,  $\tau'$ , is in phase with the strain,  $\tau' = \tau_0 \cos \delta$ , and the other out of phase component,  $\tau'' = \tau_0 \sin \delta$ .

Correspondingly, we can define two components to a "complex" modulus as,

$$G' = \frac{\tau'}{\epsilon_0} = \frac{\tau_0}{\epsilon_0} \cos \delta = G^* \cos \delta \quad (4a)$$

$$G'' = \frac{\tau''}{\epsilon_0} = G^* \sin \delta \quad (4b)$$

$$\text{Then from above, } G^* = (G'^2 + G''^2)^{1/2} \quad (5a)$$

$$\text{and } \tan \delta = G''/G' \quad (5b)$$

A more sophisticated approach with complex variables is usually used to arrive at the preceding derivations. Whence  $G^*$  is known as the complex modulus,  $G'$  as real modulus, and  $G''$  as imaginary modulus. However, it is probably more useful to retain the in-phase and out-of-phase designation so as not to lose the physical meaning of these terms.

It is possible to calculate the energy dissipated under cyclic loads in terms of the quantities just derived. The energy dissipated per cycle is simply

$$\Delta E_{\text{cycle}} = \oint \tau d\epsilon = \oint \tau \frac{d\epsilon}{dt} dt$$

Substituting Equation (2) for  $\tau$ , and differentiating Equation (3) for  $d\epsilon/dt$  and utilizing the trigonometric identity,  $\cos (\omega t - \delta) = \cos \omega t \cos \delta + \sin \omega t \sin \delta$ , Equation 6 becomes

$$\Delta E_{\text{cycle}} = \tau_0 \epsilon_0 \omega \oint \sin \omega t (\cos \omega t \cos \delta + \sin \omega t \sin \delta) dt \quad (7)$$

The first product inside the integral is an odd function and is zero over the closed integral. The second term yields  $(\pi/\omega) \sin \delta$  and the energy dissipated per cycle is given as

$$\Delta E_{\text{cycle}} = \pi \tau_0 \epsilon_0 \sin \delta \quad (8)$$

Note that for an ideally elastic material, the corresponding integral would contain only an odd-function term, in agreement with the definition that all the energy is elastically stored and none lost.

Since usually either the maximum stress or strain is an experimentally independent variable, it would be desirable to eliminate one from the expression in Equation (8). For the case when stress is constant, substitute  $\epsilon_0 = \tau_0/G^*$  and get

$$\Delta E_{\text{cycle}} = \frac{\Delta \tau_0^2}{G^*} \sin \delta \quad (9)$$

By definition, the complex compliance is  $J^* = 1/G^*$ , and correspondingly the loss compliance  $J'' = J^* \sin \delta$ . We now have arrived at a more useful expression, namely,

$$\Delta E_{\text{cycle}} = \pi \tau_0^2 J'' \quad (10)$$

Since this expression is for energy dissipated per cycle, the energy dissipation per unit time is simply,

$$\Delta E = (\pi \tau_0^2 J'')f \quad (11)$$

where  $f$  is frequency in cycles/unit time.

Let us now consider the implications of Equation (11). It is obvious that rate of energy dissipation increases rapidly with the square of peak stress and linear with the cyclic frequency. Both are experimental parameters amenable to control and measurement. The interesting parameter is the loss compliance, which is the only parameter in the equation that is a property of the polymer. We know from linear viscoelastic analysis that  $J''$  increases with temperature, increasing rapidly when the temperature approaches the glass transition or some other major transition. Dynamic mechanical measurements provide direct experimental verification within the range of linear viscoelasticity.

However, the derivation leading to Equation (11) is not strictly valid under high stress levels usually encountered in fatigue, since the response is no longer linear viscoelastic. The value of  $J''$  in the non-linear region is no longer independent of stress but increases with stress. In brief, we can only state that  $J''$  of a polymer sample under fatigue is some complicated function of temperature, frequency and stress, and Equation (11) is only an approximation.

## EXPERIMENTAL RESULTS

To our knowledge, careful dynamic mechanical characterization of polymers in the non-linear region has been rarely attempted. In particular, there are no reported data on non-linear loss compliance that would enable one to predict the extent of hysteretic heating in fatigue. In previous publications,<sup>5</sup> we made a qualitative approach to the problem. We measured the surface temperature of specimens under fatigue and compared the data to the linear loss compliance over the same temperature range. Experimental details are fully described in aforementioned references<sup>5</sup> and are not repeated here.

Figure 3 on polytetrafluoroethylene (PTFE) shows the common characteristics of the data obtained. The lower figure shows that at a stress leading to failure, the surface temperature increases gradually and then quite suddenly "runs away" just before failure. Plotting the linear dynamic loss compliance over the same tempera-

ture range in the upper figure, we find that the region where the temperature begins to run away is approximately where  $J''$  is increasing rapidly with slight changes in temperature and is approaching a transition. On the other hand, at a moderate stress level at or below the endurance limit, the surface temperature levels off to some steady-state value.

Even though the data lack decisive quantitative proof, for we did not measure the actual heat evolved nor the actual non-linear  $J''$ , the following generalizations seem justified:

1. At the experimental frequency of 30 cycles/sec., various polymers, including polymethyl methacrylate, nylon 6, polyethylene, polytetrafluoroethylene, polychlorotrifluoroethylene and polyvinylidene fluoride possess a significant loss compliance to result in appreciable hysteretic heating. Only unplasticized PVC failed by fracture without perceptible signs of heating.
2. Failure occurs when hysteretic heating from internal damping is generated at a rate faster than the rate of heat transfer to the surrounding. Since the loss compliance increases with temperature, the heating rate increases until the specimen is too soft to withstand the load and a thermal type of fatigue failure occurs. At low enough stress and/or frequency, the rate of hysteretic heating is lessened and equilibrates with the external heat transfer to attain a stable condition. Changing the surrounding environment changes the heat transfer characteristics and would also change the steady state condition that corresponds to the endurance stress level.

Hearle<sup>3</sup> suggests that "true" fatigue failure in polymers be defined as fracture due to crack growth. While this would be consistent with the classical concepts of fatigue testing, the consideration excludes the viscoelastic effects which may be too important to be ignored in practical situations.

Our experimental procedure does not separate the effects of elastic crack growth from that of hysteretic heating, and the end points reflect the combined effects. By so doing we cannot measure true S-N curves where temperature is constant, but obtain only "apparent" S-N curves. This being the case, the observed behavior can be generally separated by four regions as illustrated by Figure 4. At the highest stress levels of the diagram (Region I) the specimens tend to fracture before the specimen temperature reaches very far into the "run away" region. At intermediate stress levels (Region II), softening due to heating and evidence of melting for crystalline polymers usually takes place along with partial breakage and visible signs of crazing and small cracks. At stress levels only slightly above the endurance limit (Region III) specimens generally soften drastically. Even though such specimens are permanently weakened even when cooled back to ambient conditions, visible signs of cracking and crazing are usually absent. In Region IV below the endurance limit, the temperature reaches steady state and failure of any kind does not occur. The generalization is representative of most of the semicrystalline polymers except for PTFE which do not show any physical damage apparent to visual

inspection at any stress level, i.e., Regions I and II are not observed. The glassy PMMA, on the other hand, tend to show at least evidence of crazing even at stress levels just above the endurance limit, i.e., Region III is absent. Note that if we include fatigue fractures without any perceptible heating as part of Region I, then Figure 4 encompasses all the possible modes of fatigue behavior of high polymers. Of course, as indicated by the data on PTFE and PMMA, not all the regions are always observed for a given set of conditions. For example, at very low frequency fatigue, with no hysteretic heating, only Regions I and IV are likely to be seen.

To further explore the importance of hysteretic heating to a polymer sample under cyclic load, we then conducted a series of tests<sup>5</sup> where each test was discontinued when the specimen temperature reached a certain prescribed level below the region when failure took place. We found that even at stress levels considerably above the endurance limit, the test specimens appear capable of withstanding the cyclic load indefinitely as long as the loading is stopped before the temperature approaches the level where, based on previous continuous test data, failure occurs. This being the case, under certain practical situations where cyclic loads are applied intermittently rather than continuously, a given polymer can conceivably perform better than what the apparent S-N curves would predict. The implication is that internal structural damage within a polymer sample is caused by a combination of mechanical cyclic stress and hysteretic heating; at each stress level, there exists a critical temperature specific to each polymer below which structural damage does not appear to take place.

In order to arrive at some logical explanation for the effects observed, the next experimental phase is to conduct a microscopic examination of specimens under cyclic loads for structural and morphological changes and variations. Roldan<sup>6</sup> has done this for polytetrafluoroethylene using the optical microscope, the electron microscope, and x-ray diffraction, and is preparing the results for publication. One of the significant conclusions from his work is that crystalline bands are destroyed or at least disturbed by the combination of external stress and heating, and that cracks are initiated but are inhibited from propagating into macroscopic dimensions that lead to fracture.

If we assume that internal structural and morphological damage occurs only after the sample is at an internal state of increased molecular chain mobility, this required internal mobility would occur when the temperature of the polymer sample approached the glass transition due to hysteretic heating. It has been suggested by Andrews<sup>7</sup> and others that external stress can induce the transition to occur at a lower temperature. The relationship appears to be monotonic, i.e., greater the stress induces a greater drop in the transition temperature. Therefore, it is not necessary for the specimen under fatigue to heat up to the same temperature before internal damage takes place. Instead, damage occurs sooner, at a lower specimen temperature, for higher level of external stress as suggested by Figure 4.

A proposed explanation<sup>6</sup> for the fact that damage in PTFE does not lead to fracture, is that apparently damage occurs in the crystalline region. When the microcrack reaches the non-crystalline region, the stress concentration from the microcrack is relieved by the relaxation of the mobile chain segments.

## CONCLUSIONS

Regardless of whether hysteretic heating is a legitimate part of the classical fatigue failure or merely obscures the nature of fatigue fracture, we consider it an important consideration from a practical standpoint and cannot be ignored in many cyclic situations. A polymer with no internal damping capacity is too brittle to be a good fatigue resistant material. Polymers with sufficient damping though they may heat up are more likely to be fatigue resistant. The load bearing capability is somewhat inversely proportional to the extent of hysteretic heating, and maximum operating temperature under load is restricted to below the nearest major transition temperature above ambient - usually the glass transition temperature. External factors such as improving heat transfer, intermittent service with periods for cooling, all would tend to prolong the service life.

The microscopic examination of PTFE suggests that the weakening and failure of polymer samples under cyclic load appears to correspond to the destruction of regions of crystalline order (for semi-crystalline polymers) due to the combined effects of external stress and internal friction. Exact mechanism that relates to structure and morphology and accounts for the fatigue behavior of glassy polymers as well as crystalline polymers is an area that requires elucidation.

## ACKNOWLEDGMENT

The author wishes to acknowledge the helpful discussions and constructive comments from Drs. L. Roldan and D. Prevorsek and Mr. G. Toelke on the manuscript. Appreciation also goes to Allied Chemical Corporation, Plastics Division, for the support and permission to publish.

## REFERENCES

1. Richards, C.W., Engineering Material Science, Wadsworth, Belmont, California (1961).
2. Watts, N.H. and Burns, D.J., Polymer Eng. & Sci., 7, 90 (1967).  
Borduas, H.F., Culver, L.E. and Burns, D.J., SPE ANTEC, Vol. 13, Detroit, Michigan (May, 1967).
3. Hearle, J.W.S., J. Mtl. Sci., 2, 474 (1967).
4. Vincent, P.I., Physics of Polymers, ed. P.D. Ritchie, p. 35ff, D. van Nostrand, Princeton, N.J. (1965).
5. Riddell, M.N., Koo, G.P. and O'Toole, J.L., Polymer Eng. & Sci., 6, 363 (1966).  
Koo, G.P., Riddell, M.N. and O'Toole, J.L., Polymer Eng. & Sci., 7, 182 (1967).
6. Roldan, L.G. and Koo, G.P., to be published.
7. Andrews, R.D. and Hammack, T.J., Polymer Letters, 3, 655 (1965).  
Andrews, R.D., J. Polymer Sci., C14, 261 (1966).  
Andress, R.D., and Kazama, Y., J. Appl. Phys., 38, 4118 (1967).

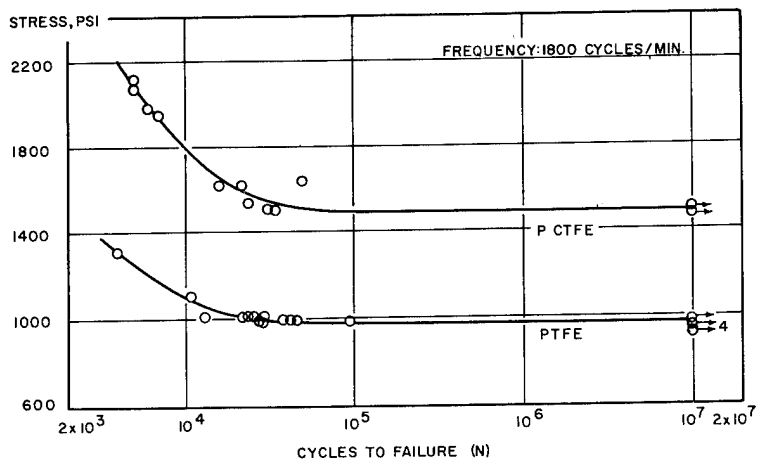


FIGURE 1: Typical stress versus fatigue life, S-N curves given for polychlorotrifluoroethylene and polytetrafluoroethylene at 30 cycles/sec.

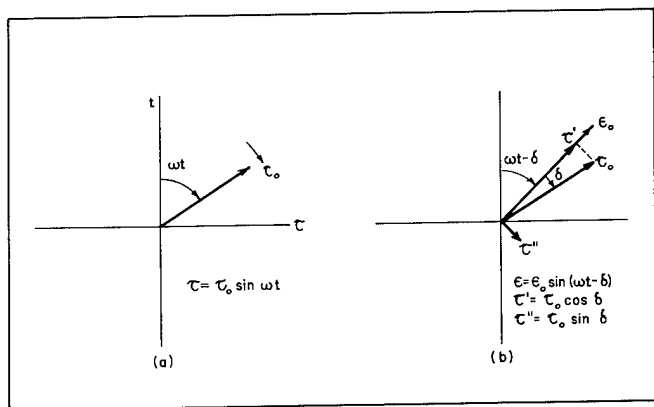


FIGURE 2: Relationship between stress, strain and phase angle of a linear viscoelastic body under sinusoidal oscillation.

FIGURE 3: Characteristic temperature rise during fatigue and the variation in loss compliance over the same temperature range. Given for polytetrafluoroethylene.

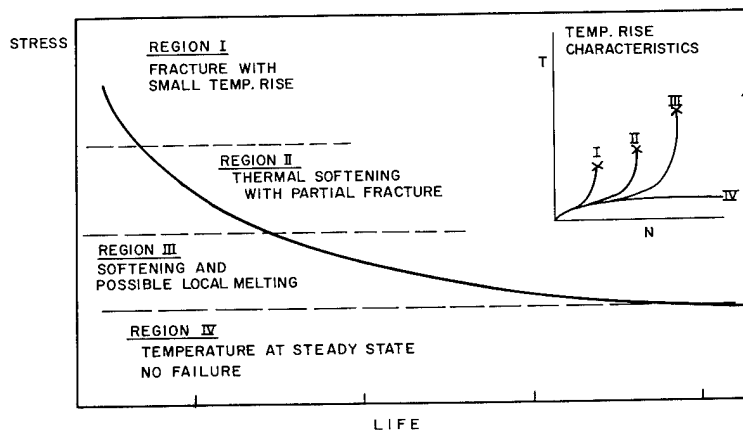
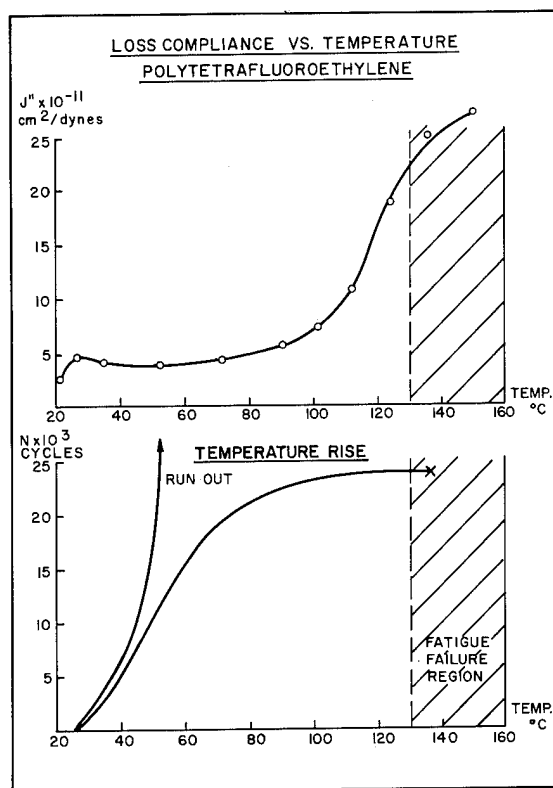


FIGURE 4: Generalized regions of fatigue behavior observed in polymers.

**INITIATION FEE  
MUST BE ATTACHED  
FOR PROCESSING.**



**SOCIETY OF PLASTICS ENGINEERS, INC.**

65 Prospect Street, Stamford, Conn. 06902  
348-7528 AREA CODE 203

## MEMBERSHIP APPLICATION

**PLEASE PRINT OR TYPE**

**Executive Office Use Only**

I.D. No. \_\_\_\_\_

Ack. \_\_\_\_\_

Elected \_\_\_\_\_

I hereby make application for { ☐ admission into  
☐ reclassification within  
☐ reinstatement in } the Society of Plastics Engineers, Inc. in the grade of membership indicated below for which I believe I am qualified  
(See instructions or reverse side.)

Grade	Initiation Fees	Annual Dues	Foreign Dues	I wish to affiliate with the _____
<input type="checkbox"/> Senior Member	\$10.00	\$20.00	\$17.50	_____
<input type="checkbox"/> Member	10.00	20.00	17.50	_____
<input type="checkbox"/> Affiliate Member	10.00	20.00	17.50	_____ section _____
<input type="checkbox"/> Student Member	None	5.00	5.00	(Geographical location. See listing on reverse side.)

Applicants Full Name \_\_\_\_\_  
(First) (M.I.) (Last) (Citizen of) (Birthdate)

Please fill in both addresses and **CHECK THE ONE TO WHICH YOUR MAIL SHOULD BE ADDRESSED.**

☐ **BUSINESS:** Company Name and Division: \_\_\_\_\_

Position \_\_\_\_\_

Address \_\_\_\_\_ City \_\_\_\_\_ State \_\_\_\_\_ Zip Code \_\_\_\_\_

☐ **HOME:** Address \_\_\_\_\_ City \_\_\_\_\_ State \_\_\_\_\_ Zip Code \_\_\_\_\_

**REFERENCES** The By-Laws require the names of three references who are familiar with your work. One of them should be a member of the Society. Assistance in providing member-references, when needed, will be given on request.

1. \_\_\_\_\_ Address \_\_\_\_\_

2. \_\_\_\_\_ Address \_\_\_\_\_

3. \_\_\_\_\_ Address \_\_\_\_\_

### STATEMENT OF COLLEGE WORK

Years Attended		Institution	Major and Minor	Degree	Experience Credits See reverse side
From	To				
Total Education Experience Credits					

### RECORD OF QUALIFYING EXPERIENCE IN PLASTICS

Dates				Give your title, name and location of employer, and name of immediate superior for each position. List in chronological order. Describe duties fully and state briefly any important engineering work you have done in in each position. If space is not sufficient, use a separate sheet.	Time in years and months
From		To			
Mo.	Yr.	Mo.	Yr.		

I certify that the statements made in this application are correct. I agree, if elected, to be governed by the Constitution and By-Laws of the Society, and to promote the objective of the Society.

**Total qualifying years of experience.**

**Total education and qualifying experience credits.**

NATIONAL CREDENTIALS COMMITTEE USE ONLY

**Approved (Signature)**

Date \_\_\_\_\_

Approved (Signature)

Date \_\_\_\_\_

Date of Application

Signature in ink.

# COMPLETING THE APPLICATION

## Grade of Membership . . .

Membership grades are based on experience credits which are earned as follows:

### 1. Experience credits earned for education.

Doctorate in science or engineering subject: **6 credits**  
Masters in science or engineering subject: **5 credits**  
Bachelors in science or engineering subject: **4 credits**  
Other degree in non-science or non-engineering subject: **2 credits**

Maximum credits allowable for education shall be six (6).  
When filling in the "Statement of College Work" on the reverse side of this application, please place the corresponding number of credits earned in the right-hand column.

### 2. Experience credits for qualifying experience in plastics or plastics engineering are earned at the rate of one (1) per year, e.g. 5½ years of qualifying experience = 5½ credits. Please detail carefully the engineering skill required for each position to help the Credentials Committee judge experience as "qualifying."

When filling in the "Record of Qualifying Experience in Plastics" on the reverse side, please place the amount of time spent in each position (in years and months) in the right-hand column.

When you have determined the number of credits which you believe you have earned consult the following membership grade requirements. Indicate on the reverse side the grade of membership for which you believe you are qualified.

GRADE	REQUIREMENTS
Senior Member	Minimum of twelve (12) experience credits and maintained continuous membership in the Society for a minimum of two (2) years.
Member	Minimum of six (6) experience credits
Affiliate Member	Less than six (6) experience credits
Student Member	Regularly enrolled student (full- or part-time) in a course of study in plastics and between the ages of 16 years and 26 years, inclusive.

## THIS PORTION MUST BE COMPLETED FOR PROCESSING OF YOUR APPLICATION.

Please check off the principal activity of your company under either Manufacturing or Non-Manufacturing.

### MANUFACTURING

1. ☐ Electrical & Electronic Machinery, Equipment & Appliances
2. ☐ Motor Vehicles and Equipment
3. ☐ Transportation Equipment (except Motor Vehicles)
4. ☐ Professional, Scientific and Controlling Instruments, Photographic & Optical Goods, Clocks
5. ☐ Iron, Steel & Nonferrous Metals & Machinery (except Plastic & Electrical Machinery)
6. ☐ Fabricated Metal Products and Housewares
7. ☐ Finished Apparel Products
8. ☐ Food and Tobacco Products
9. ☐ Toilet Preparations, Drugs and Insecticides
10. ☐ Paints, Varnishes, and Industrial Chemicals (except Plastic Raw Materials)
11. ☐ Petroleum, Coal, Rubber, Stone and Glass Products
12. ☐ Musical Instruments, Toys, Sporting Goods, Athletic Goods, Ordnance & Smokers' Supplies
13. ☐ Jewelry and Fashion Accessories
14. ☐ Furniture and Finished Wood Products
15. ☐ Leather and Leather Products
16. ☐ MANUFACTURING, other than above. Please specify \_\_\_\_\_

17. ☐ Plastics Custom Molders, Extruders, Laminators, and Fabricators
18. ☐ Plastic Materials
19. ☐ Producers and Processors of Textiles, Lumber, Paper, Oils, Dyes, Chemicals, etc. used in Manufacture of Plastics
20. ☐ Plastic Machinery

### NON-MANUFACTURING

21. ☐ Government: Federal, State, Municipal and Foreign; Officers of the Armed Forces
22. ☐ Advertising Agencies, Sales Consultants and Sales Engineers
23. ☐ Libraries, Schools, Colleges and Trade Associations
24. ☐ Consultants and Research Organizations, Architects, Engineers, Designers, Chemists
25. ☐ Transportation Operating Companies
26. ☐ Retail Stores
27. ☐ Exporters, Importers, Distributors, Jobbers, Wholesalers and Manufacturers' Agents
28. ☐ Doctors, Lawyers and other Professionals
29. ☐ NON-MANUFACTURING, other than above. Please specify \_\_\_\_\_
30. ☐ Packaging & Containers
31. ☐ Aerospace
32. ☐ Construction Materials



# MEMBERSHIP APPLICATION

**SOCIETY OF PLASTICS ENGINEERS, INC.**  
65 Prospect Street, Stamford, Conn. 06902  
348-7528 AREA CODE 203

## SPE SECTIONS

AKRON	NORTHERN INDIANA
ARIZONA	NORTHWEST
BALTIMORE	PENNSYLVANIA
WASHINGTON	OMAHA
BARTLESVILLE-TULSA	ONTARIO
BINGHAMTON	PACIFIC NORTHWEST
BUFFALO	PALSADES
CENTRAL INDIANA	PHILADELPHIA
CENTRAL NEW YORK	PIONEER VALLEY
CENTRAL OHIO	PITTSBURGH
CHICAGO	QUEBEC
CLEVELAND	ROCHESTER
CONNECTICUT	ROCK VALLEY
DELAWARE VALLEY	ROCKY MOUNTAIN
DETROIT	ST. LOUIS
EAST CENTRAL	SOUTH TEXAS
ILLINOIS	SOUTHEASTERN OHIO
EASTERN NEW ENGLAND	SOUTHERN
FLORIDA	SOUTHERN CALIFORNIA
GOLDEN GATE	SOUTHEASTERN NEW ENGLAND
HUDSON-MOHAWK	SOUTHWEST VIRGINIA
JAPAN	TENNESSEE VALLEY
KANSAS CITY	TOLEDO
KENTUCKIANA	TRI STATE
MIAMI VALLEY	UPPER MIDWEST
MID-MICHIGAN	VIRGINIA-CAROLINA
MILWAUKEE	WESTERN MICHIGAN
MONTEREY	WESTERN NEW ENGLAND
NEW YORK	NEWARK
NORTH TEXAS	NON-SECTION